GENERAL QUESTIONS OF THERMODYNAMICS, STATISTICAL PHYSICS, AND QUANTUM MECHANICS

EQUATION OF STATE FOR THE TWO-COMPONENT VAN DER WAALS GAS WITH RELATIVISTIC EXCLUDED VOLUMES

G. ZEEB, K.A. BUGAEV[1], P.T. REUTER[2], H. STÖCKER

Institut für Theoretische Physik, J.-W.-Goethe Universität, Frankfurt am Main
(1, Max von Laue Str., Frankfurt am Main 60438, Germany; e-mail: gzeeb@th.physik.uni-frankfurt.de),

[1]**Bogolyubov Institute for Theoretical Physics, Nat. Acad. Sci. of Ukraine**
(14b, Metrologichna Str., Kyiv 03680, Ukraine; e-mail: bugaev@th.physik.uni-frankfurt.de),

[2]**Triumf, Canada**
(4004, Wesbrook Mall, Vancouver, Canada V6T 2A3; e-mail: reuter@triumf.ca)

UDC 539.12

A canonical partition function for the two-component excluded volume model is derived, leading to two different van der Waals equations of state. The one of them is known as the Lorentz–Berthelot mixture, and the other has been proposed recently. Both models are analyzed in the canonical and grand canonical ensembles. In comparison with the one-component van der Waals excluded volume model, the suppression of particle densities is reduced in these two-component formulations, but in two essentially different ways. Presently used multicomponent models have no such reduction. They are shown to be not correct when used for the mixture of particles with different hard-core radii.

For high temperatures, the excluded volume interaction is refined by accounting for the Lorentz contraction of the spherical excluded volumes, which leads to a distinct enhancement for the light particle contributions into thermodynamic functions. The resulting influence of two hard-core radii and Lorentz contraction on pion and nucleon yields is studied in detail for AGS and SPS data.

1. Introduction

Thermal models are commonly used to interpret experimental data on hadron collisions, see, for instance, [1–5]. In the van der Waals (VdW) excluded volume model, the short-range repulsion between particles is represented by hard-core potentials, i. e. the finite size of the particles is taken into account. As a consequence, the particle yields are essentially reduced compared to the ideal gas results, whereas yield ratios remain almost unchanged, if the same hard-core radius is used for all particle species.

As particle species with smaller hard-core radii are closer to the ideal case, their particle densities are suppressed less. Consequently, their yield ratios to particle species with larger hard-core radii are enhanced. This fact has been used in recent attempts [6] to explain the experimentally observed pion abundance for AGS and SPS data [7] by introducing a smaller hard-core radius for pions R_π than for all other hadrons R_0. However, the resulting values of radii are quite large, $R_0 = 0.8$ fm and $R_\pi = 0.62$ fm. On the other hand, a reasonable fit of SPS data has been obtained in [8] only for a distinctly smaller pair of hard-core radii.

However, the excluded volume models used in [6, 8] are not correct in the case of different hard-core radii. As will be shown in Sect. 2, these models correspond to a system where the components are separated from each other by a mobile wall and hence cannot mix.

A more realistic approach requires a two-component partition function including a term for the repulsion between particles of different hard-core radii. In the case of two components, however, the VdW approximation is not uniquely defined. The simplest possibility yields the Lorentz–Berthelot mixture, which was originally postulated by van der Waals for binary mixtures,

see [9–12]. Another VdW approximation was recently proposed in [13]. These two formulations contain a suppression of particle densities similar to the one-component van der Waals gas, which is reduced to different extent for each formulation. In the present work, we will study and apply both of these formulations.

There is yet another cause for a reduced excluded volume suppression. Particles are considered to be rigid spheres in the VdW model. At high energies as achieved in nuclear collisions, however, relativistic effects cannot be neglected [14]. Within the logic of the VdW model, it is necessary to take the Lorentz contraction of hard spheres into account. The inclusion of the Lorentz contraction is not only required by special relativity which forbids the existence of hard bodies, but it is also demanded by the practical necessity to describe the properties of hadrons above the cross-over transition. The lattice quantum chromodynamics simulations [15, 16] predict the coexistence of usual hadrons and quark-gluon plasma for the temperatures of about 2 to 3 values of the cross-over temperature at zero value of the baryonic chemical potential. Therefore, to describe the strongly interacting matter properties above the cross-over region within the phenomenological approach [17], the Lorentz contraction should be accounted not only for pions, but also for kaons, ω and ρ mesons, and even for heavier hadrons, if they do not melt at higher temperatures.

For this purpose, we will use an approach developed in [18] providing approximative formulae for relativistic excluded volumes: naturally, they decrease with rising temperature, and the effect is stronger for lighter particles. At high temperatures, consequently, it is not possible to use a one-component VdW description (i. e. a common excluded volume for all particle species) for a system of species with various masses. Since different masses cause different reductions of the excluded volumes at a given temperature, a multicomponent VdW description is required.

To illustrate the influence of different excluded volumes, we will restrict ourselves in this work to the simplest 'multicomponent' case, the two-component case. The crucial extension from the one- to the two-component case is to include the repulsion between particles of two different hard-core radii. As it will be illustrated, a generalization to the multicomponent case is straightforward and will yield no essential differences [19].

In the next section, a derivation of the one-component canonical partition function with (constant) excluded volumes is presented. The generalization to the two-component case is made, and two possible VdW approximations are analyzed: the Lorentz–Berthelot mixture [12] and the recently proposed approximation in [13]. The corresponding formulae for the grand canonical ensemble are derived and discussed in Sect. 3. Relativistic excluded volumes are introduced in Sect. 4, and the corresponding equations of state are presented for both models. In Sect. 5, a fit of particle yield ratios [6] is re-evaluated for both approximations, with constant and with relativistic excluded volumes. The conclusions are given in Sect. 6.

The Appendices A–C give a detailed analysis and a comparison of the two approximations in the canonical and grand canonical ensembles, respectively. In App. B, a general proof of the thermodynamical stability of the non-linear approximation is given.

2. Canonical Treatment

First we will derive the canonical partition function (CPF) for the one-component VdW gas by estimating the excluded volumes of particle clusters. Then this procedure will be generalized to the two-component case.

For simplicity, the Boltzmann statistics are used throughout this work. The deviations from quantum statistics are negligible as long as the density over temperature ratio is small. This is the case for the hadron gas at temperatures and densities typical of heavy ion collisions, see e. g. [6].

Note that, in this work, we will use the term VdW for the van der Waals excluded volume model, not for the general van der Waals model which includes attraction.

2.1. The Van der Waals excluded volume model

Let us consider N identical particles at temperature T kept in a sufficiently large volume V, so that finite volume effects can be neglected. The partition function of this system ($\hbar = c = k_{\mathrm{B}} = 1$) reads

$$Z(T,V,N) = \frac{\phi^N}{N!} \int_{V^N} \mathrm{d}^3x_1 \, \cdots \, \mathrm{d}^3x_N \, \exp\left[-\tfrac{U_N}{T}\right] \, . \quad (1)$$

Here, $\phi \equiv \phi(T;m,g)$ denotes the momentum integral of the one-particle partition

$$\phi(T;m,g) = \frac{g}{2\pi^2} \int\limits_0^\infty \mathrm{d}k \, k^2 \, \exp\left[-\tfrac{E(k)}{T}\right] \, , \quad (2)$$

where $E(k) \equiv \sqrt{k^2+m^2}$ is the relativistic energy and $g = (2S+1)(2I+1)$ counts the spin and isospin

degeneracy. For a hard-core potential U_N of N spherical particles with radii R, the potential term in Eq. (1) reads

$$\exp\left[-\tfrac{U_N}{T}\right] = \prod_{i<j\le N} \theta(|\vec{x}_{ij}| - 2R) \ , \qquad (3)$$

where $\vec{x}_{ij}$ denotes the relative position vector connecting the centers of the i-th and j-th particles. Hence one can write

$$\int_{V^N} \mathrm{d}^3x_1 \ \cdots \ \mathrm{d}^3x_N \ \exp\left[-\tfrac{U_N}{T}\right] = \int_{V^N} \mathrm{d}^3x_1 \ \cdots \ \mathrm{d}^3x_N \times$$

$$\times \prod_{1\le i<j\le N} \theta(|\vec{x}_{ij}| - 2R) = \int_V \mathrm{d}^3x_1 \int_V \mathrm{d}^3x_2 \ \theta(|\vec{x}_{12}| - 2R) \times$$

$$\times \ \cdots \int_V \mathrm{d}^3x_N \prod_{1\le i\le N-1} \theta(|\vec{x}_{i,N}| - 2R) \equiv$$

$$\equiv \int_V \mathrm{d}^3x_1 \int^{\{\vec{x}_1\}} \mathrm{d}^3x_2 \ \cdots \int^{\{\vec{x}_1 \ldots \vec{x}_{N-1}\}} \mathrm{d}^3x_N \ . \qquad (4)$$

Here, $\int^{\{\vec{x}_1 \ldots \vec{x}_j\}} \mathrm{d}^3x_{j+1}$ denotes the available volume for $\vec{x}_{j+1}$, which is the center of the particle with number $j+1$, if the j other particles are configurated as $\{\vec{x}_1 \ldots \vec{x}_j\}$. We will show now that this volume is estimated by $\int^{\{\vec{x}_1 \ldots \vec{x}_j\}} \mathrm{d}^3x_{j+1} \ge (V - 2b\,j)$, where $2b \equiv \frac{4\pi}{3}(2R)^3$ is the excluded volume of an isolated particle seen by a second one. Then, $2b\,j$ estimates the total volume which is excluded by all particle clusters occuring in the configuration $\{\vec{x}_1 \ldots \vec{x}_j\}$.

It is sufficient to prove that the excluded volume of a cluster of k particles is less than the excluded volume of k isolated particles. A group of k particles forms a k-cluster, if, for any of these particles, there is a neighbouring particle of this group at a distance less than $4R$. The exact excluded volume of a k-cluster, $v_{(k)}$, obviously depends on the configuration of k particles. If one considers two isolated particles, i. e. two 1-clusters, and reduces their distance below $4R$, their excluded volumes will overlap. They form now a 2-cluster with the excluded volume $v_{(2)} = 4b - 1v_{\mathrm{ov}}$, where v_{ov} denotes the overlap volume.

Evidently, one can construct any k-cluster by attaching additional particles and calculate its excluded volume by subtracting each occuring overlap volume from $2b\,k$. It follows that $v_{(k)} < 2b\,k$ is valid for any k-cluster, and this inequality leads to the above estimate. Obviously, its accuracy improves with the diluteness of the gas.

Using these considerations, one can approximate the r. h. s. of Eq. (4) : starting with $j+1 = N$, one gradually replaces all integrals $\int^{\{\vec{x}_1 \ldots \vec{x}_j\}} \mathrm{d}^3x_{j+1}$ by $(V - 2b\,j)$. One has to proceed from the right to the left, because only the respective rightmost of these integrals can be estimated in the described way. Hence one finds

$$Z(T,V,N) \ge \frac{\phi^N}{N!} \prod_{j=0}^{N-1} (V - 2b\,j) \ . \qquad (5)$$

In this treatment, the VdW approximation consists of two assumptions concerning Eq. (5). Firstly, the product can be approximated by

$$\prod_{j=0}^{N-1} \left(1 - \tfrac{2b}{V}\,j\right) \cong \exp\left[-\textstyle\sum_{j=0}^{N-1} \frac{2b}{V}\,j\right] =$$

$$= \exp\left[-\tfrac{b}{V}\,(N-1)N\right] \cong \left(1 - \tfrac{b}{V}\,N\right)^N \ , \qquad (6)$$

where $\exp[-x] \cong (1-x)$ is used for dilute systems, i. e. for low densities $2bN/V \ll 1$. The second assumption is to take the equality instead of the inequality in Eq. (5). Then the CPF takes the VdW form,

$$Z_{\mathrm{VdW}}(T,V,N) = \frac{\phi^N}{N!}\ (V - bN)^N \ . \qquad (7)$$

As usual, the VdW CPF is obtained as an approximation for dilute systems, but, when used for high densities, it should be considered as an extrapolation.

Finally, one obtains the well-known VdW pressure formula from the thermodynamical identity $p(T,V,N) \equiv T\,\partial \ln[Z(T,V,N)]/\partial V$,

$$p_{\,\mathrm{VdW}}(T,V,N) = \frac{T\,N}{V - bN} \ , \qquad (8)$$

using the logarithm of the Stirling formula.

Now let us briefly investigate a system of volume V containing two components with different hard-core radii R_1 and R_2 which are separated by a wall and occupy the volume fractions xV and $(1-x)V$, respectively. According to Eq. (8), their pressures read

$$p_{\,\mathrm{VdW}}(T, xV, N_1) = \frac{T\,N_1}{xV - N_1 b_{11}} \ , \qquad (9)$$

$$p_{\,\mathrm{VdW}}(T, (1-x)V, N_2) = \frac{T\,N_2}{(1-x)V - N_2 b_{22}} \ , \qquad (10)$$

where the particle numbers N_1, N_2 and the excluded volumes $b_{11} = \frac{16\pi}{3}\,R_1^3$, $b_{22} = \frac{16\pi}{3}\,R_2^3$ correspond to components 1 and 2, respectively.

If the separating wall is mobile, pressures (9) and (10) must be equal. In this case, the fraction x can be

eliminated, and one obtains the common pressure of the whole system

$$p_{\,\mathrm{VdW}}(T, xV, N_1) = p_{\,\mathrm{VdW}}(T, (1-x)V, N_2) =$$

$$= p^{\,\mathrm{sp}}(T, V, N_1, N_2) \equiv \frac{T\,(N_1+N_2)}{V - N_1 b_{11} - N_2 b_{22}}\ . \qquad (11)$$

Since the components are separated in this model system, it will be referred to as the separated model [19].

The pressure formula (11) corresponds to the Boltzmann approximation of the commonly used two-component VdW models of [6, 8] as will be shown in Sect. 5. It is evident that $p^{\,\mathrm{sp}}$ (11) does not describe the general two-component situation without a separating wall. Therefore, it is necessary to find a more realistic model, i. e. an approximation from a two-component partition function. This will be done in the following.

2.2. Generalization to the two-component case

Recall the simple estimate (4)–(7) which gives a physically transparent derivation of the one-component CPF in the VdW approximation. Let us use it now for a two-component gas of spherical particles with radii R_1 and R_2, respectively. It is important to mention that each component may consist of several particle species as long as these species have one common hard-core radius, i. e. the number of necessary VdW components is determined by the number of different excluded volume terms b_{qq}. In the case of two radii, the potential term (3) becomes

$$\exp\left[-\tfrac{U_{N_1+N_2}}{T}\right] = \prod_{i<j\le N_1} \theta(|\vec{x}_{ij}| - 2R_1)\times$$

$$\times \prod_{k<\ell\le N_2} \theta(|\vec{x}_{k\ell}| - 2R_2) \prod_{\substack{m\le N_1\\ n\le N_2}} \theta(|\vec{x}_{mn}| - (R_1+R_2))\ . \qquad (12)$$

The integration is carried out in the way described above; e. g. firstly over the coordinates of the particles of the second component, then over those of the first component. For the estimation of the excluded volume of a k-cluster, two different particle sizes have to be considered. One obtains

$$Z(T, V, N_1, N_2) \ge \frac{\phi_1^{N_1}}{N_1!}\,\frac{\phi_2^{N_2}}{N_2!} \left\{\prod_{i=0}^{N_1-1} (V - 2b_{11}\,i)\right\}\times$$

$$\times \left\{\prod_{j=0}^{N_2-1} (V - 2b_{12}\,N_1 - 2b_{22}\,j)\right\} \cong \frac{\phi_1^{N_1}}{N_1!}\,\frac{\phi_2^{N_2}}{N_2!}\times$$

$$\times V^{N_1+N_2} \exp\left[-\tfrac{{N_1}^2 b_{11} + 2N_1N_2 b_{12} + {N_2}^2 b_{22}}{V}\right]\ , \qquad (13)$$

where it is $\phi_q \equiv \phi(T; m_q, g_q)$, and $2b_{pq} \equiv \frac{4\pi}{3}(R_p + R_q)^3$ denotes the excluded volume of a particle of the component p seen by a particle of the component q ($p,\ q = 1, 2$ hereafter). Approximating the above exponent by $\exp[-x] \cong (1-x)$ yields the simplest possibility of a VdW approximation for the two-component CPF,

$$Z^{\,\mathrm{nl}}_{\mathrm{VdW}}(T, V, N_1, N_2) \equiv \frac{\phi_1^{N_1}}{N_1!}\,\frac{\phi_2^{N_2}}{N_2!}\times$$

$$\times \left(V - \frac{{N_1}^2 b_{11} + 2N_1N_2 b_{12} + {N_2}^2 b_{22}}{N_1+N_2}\right)^{N_1+N_2} =$$

$$= \frac{\phi_1^{N_1}}{N_1!}\,\frac{\phi_2^{N_2}}{N_2!} \left(V - N_1 b_{11} - N_2 b_{22} + \frac{N_1\,N_2}{N_1+N_2}\,D\right)^{N_1+N_2}\ , \qquad (14)$$

where the non-negative coefficient D is given by

$$D \equiv b_{11} + b_{22} - 2\,b_{12}\ . \qquad (15)$$

This approximation will be called the non-linear approximation as the volume correction in (14) contains non-linear terms in N_1, N_2. The corresponding pressure follows from the thermodynamical identity

$$p^{\,\mathrm{nl}}(T, V, N_1, N_2) = p_1^{\,\mathrm{nl}} + p_2^{\,\mathrm{nl}} \equiv$$

$$\equiv \frac{T\,(N_1+N_2)}{V - N_1 b_{11} - N_2 b_{22} + \frac{N_1\,N_2}{N_1+N_2}\,D}\ . \qquad (16)$$

This canonical formula corresponds to the Lorentz–Berthelot mixture (without attraction terms) known from the theory of fluids [12]. It was postulated by van der Waals [9] and studied as well by Lorentz [10] and Berthelot [11].

The crucial step from the one- to the two-component gas is to include b_{pq} terms ($p \ne q$) additionally to the $b_{qq} \equiv b|_{R=R_q}$ terms. For the multicomponent gas, no further essential extension is necessary. Consequently, the generalization of the above procedure to the multicomponent case, i. e. an arbitrary number of different hard-core radii, is straightforward [19].

In [13] a more involved approximation has been suggested for the two-component VdW gas. This follows from splitting the exponent in the CPF (13) by introducing two generalized excluded volume terms $\tilde{b}_{12}$ and $\tilde{b}_{21}$ (instead of a single and symmetric term $2\,b_{12}$) for the mixed case,

$$Z(T, V, N_1, N_2) \cong \frac{\phi_1^{N_1}}{N_1!}\,\frac{\phi_2^{N_2}}{N_2!}\ V^{N_1+N_2}\times$$

$$\times \exp\left[-\frac{N_1{}^2 b_{11}+N_1 N_2\left(\tilde{b}_{12}+\tilde{b}_{21}\right)+N_2{}^2 b_{22}}{V}\right] , \qquad (17)$$

which leads to an alternative two-component VdW CPF

$$Z_{\mathrm{VdW}}^{\mathrm{lin}}(T,V,N_1,N_2) \equiv \frac{\phi_1^{N_1}}{N_1!}\left(V-N_1 b_{11}-N_2\tilde{b}_{21}\right)^{N_1} \times$$

$$\times \frac{\phi_2^{N_2}}{N_2!}\left(V-N_2 b_{22}-N_1\tilde{b}_{12}\right)^{N_2} . \qquad (18)$$

Since the particle numbers N_1, N_2 appear solely linearly in the volume corrections, these formulae will be referred to as the linear approximation. In this approximation, the pressure is given by the formula [13]

$$p^{\,\mathrm{lin}}(T,V,N_1,N_2) \;=\; p_1^{\mathrm{lin}}+p_2^{\mathrm{lin}} \equiv$$

$$\equiv \frac{T\,N_1}{V-N_1 b_{11}-N_2\tilde{b}_{21}}+\frac{T\,N_2}{V-N_2 b_{22}-N_1\tilde{b}_{12}} . \qquad (19)$$

The choice of the generalized excluded volume terms $\tilde{b}_{pq}$ is not unique in the sense that all choices which satisfy the basic constraint $\tilde{b}_{12}+\tilde{b}_{21} = 2b_{12}$ are consistent with the second-order virial expansion [13]. Therefore, additional conditions are necessary to fix these generalized excluded volumes. In [13], they were chosen as

$$\tilde{b}_{12} \equiv b_{11}\,\frac{2\,b_{12}}{b_{11}+b_{22}} , \qquad \tilde{b}_{21} \equiv b_{22}\,\frac{2\,b_{12}}{b_{11}+b_{22}} . \qquad (20)$$

For this choice, the linear approximation reproduces a traditional VdW gas behavior, i. e. one-component-like, in the two limits $R_2 = R_1$ and $R_2 = 0$, as readily checked. The factor $2b_{12}/(b_{11}+b_{22}) = 1-D/(b_{11}+b_{22})$ is always smaller than unity for $R_1 \neq R_2$, consequently, the $\tilde{b}_{pq}$ terms are smaller than the corresponding terms b_{pp}. Note that there are many possible choices for $\tilde{b}_{12}$ and $\tilde{b}_{21}$, e. g. additionally dependent on the particle numbers N_1 and N_2, whereas the non-linear approximation (14) contains no such additional parameters.

The formulae of the linear approximation are generally valid for any choice of $\tilde{b}_{12}$ and $\tilde{b}_{21}$ satisfying the constraint $\tilde{b}_{12}+\tilde{b}_{21} = 2b_{12}$. In the following, however, we will restrict our study to the special choice given in Eqs. (20). The canonical (and grand canonical) formulae for the multicomponent case are given in [13].

2.3. Comparison of both two-component VdW approximations

As the VdW approximation is a low density approximation, it is evident that the linear and non-linear formulae are equivalent for such densities. Deviations, however, occur at high densities, where any VdW approximation generally becomes inadequate.

The differences between both approximations result from the fact that the linear pressure (19) has two poles, $v_1^{\mathrm{lin}} = V$ and $v_2^{\mathrm{lin}} = V$, whereas the non-linear pressure (16) has solely one pole, $v^{\,\mathrm{nl}} = V$. For constant volume V, these poles define limiting densities, e. g., $\hat{n}_1 = \max(N_1/V)$ as functions of $n_2 = N_2/V$,

$$v_q^{\,\mathrm{lin}}(N_1,N_2) = V \quad \rightsquigarrow \quad \hat{n}_1(n_2) \equiv \hat{n}_{1,q}^{\,\mathrm{lin}}(n_2) \qquad (21)$$

or

$$v^{\,\mathrm{nl}}(N_1,N_2) = V \quad \rightsquigarrow \quad \hat{n}_1(n_2) \equiv \hat{n}_1^{\,\mathrm{nl}}(n_2) , \qquad (22)$$

which represent the domains of two pressure formulae in the n_2–n_1-plane. The explicit fomulae are discussed in App. A.

In Fig. 1,*a*, an example of these limiting densities is shown for $R_2/R_1 = 0.4$. It is clearly seen that the non-linear domain (below the solid line) is larger than the linear domain (below both dashed lines), which is generally the case for $R_2 \neq R_1$. Especially for $R_2 \ll R_1$, the non-linear domain is distinctly larger for high densities of the large component, $n_1 b_{11} > n_2 b_{22}$, whereas both domains are similar for high densities of the small component, $n_2 b_{22} > n_1 b_{11}$.

The linear approximation is constructed in the traditional VdW spirit; the densities n_q^{lin} achieved in this approximation are below the maximum density of the corresponding one-component VdW gas $\max(n_q^{\mathrm{oc}}) = 1/b_{qq}$, which is defined by the pole of $p_q^{\mathrm{oc}} \equiv p_{\,\mathrm{VdW}}(T,V,N_q;b_{qq})$ from Eq. (8).

In the non-linear approximation, however, the possible densities of the larger particles n_1^{nl} can exceed $1/b_{11}$ due to the occurence of negative partial derivatives of the pressure, $\partial p^{\,\mathrm{nl}}/\partial N_2 < 0$. In this context, it is necessary to state that this behavior does not lead to a thermodynamical instability of the non-linear approximation as proven in App. B. The linear approximation shows no such behavior, it is always $\partial p^{\,\mathrm{lin}}/\partial N_1 > 0$ and $\partial p^{\,\mathrm{lin}}/\partial N_2 > 0$.

The condition $\partial p^{\,\mathrm{nl}}/\partial N_2 = 0$ defines the boundary $\hat{n}_1^{\,\mathrm{nl,\,bd}}(n_2)$ of the region of negative partial derivatives of the non-linear pressure. In Fig. 1,*a*, this boundary is shown by the dotted line for $R_2/R_1 = 0.4$; the values of $\partial p^{\,\mathrm{nl}}/\partial N_2$ are negative above this line.

Densities larger than $n_1^{\mathrm{nl}} = 1/b_{11}$ can only occur, if R_2 is smaller than a critical radius,

$$R_2 < R_{2,\,\mathrm{crit}}(R_1) = (\sqrt[3]{4}-1)\,R_1 \approx R_1/1.7 . \qquad (23)$$

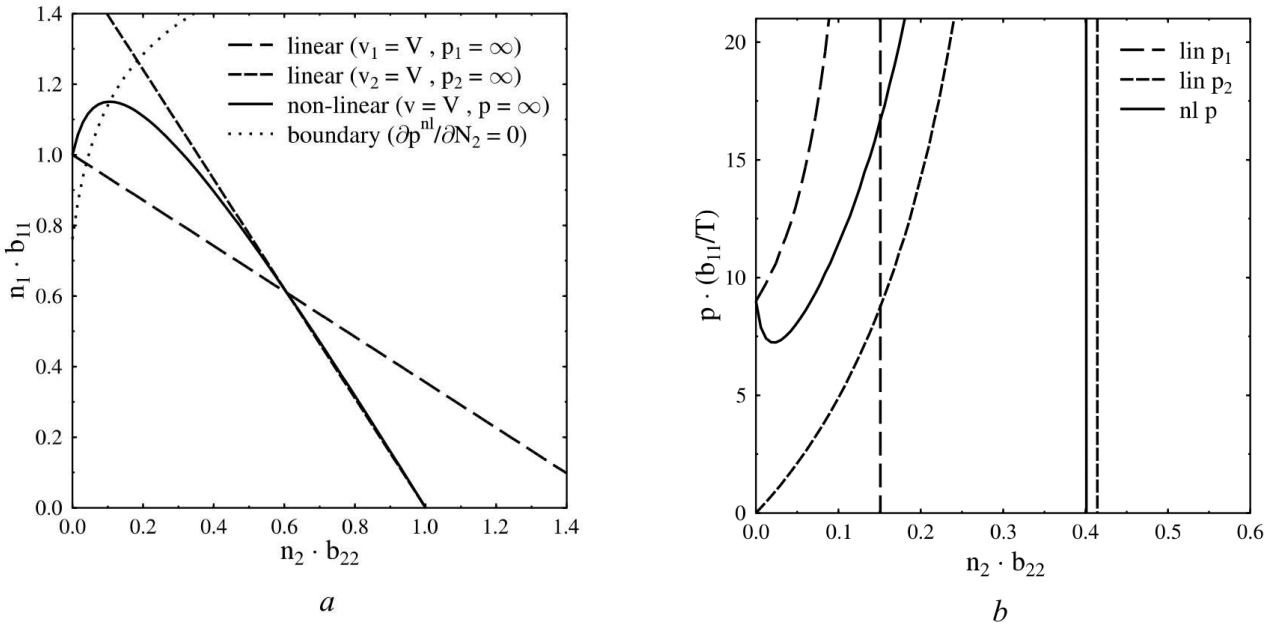

Fig. 1. *a* – domains of the linear and non-linear approximations for $R_2/R_1 = 0.4$: limiting densities $\hat{n}_1$ (isobars for $p_q(n_1, n_2) = \infty$) and the lower boundary $\hat{n}_1^{\mathrm{nl,\,bd}}$ to the region of negative partial derivatives of the non-linear pressure. The dashed lines correspond to the two poles of the linear pressure, and the solid line corresponds to the pole of the non-linear pressure. For given n_2, the possible densities n_1^{lin} are below both dashed lines, whereas the possible densities n_1^{nl} are below the solid line. Negative derivatives $\partial p^{\mathrm{nl}}/\partial N_2 < 0$ occur only above the dotted line. *b* – pressure profiles in dimensionless units for $R_2/R_1 = 0.4$ as in (*a*) at fixed $n_1 b_{11} = 0.9$. The dashed lines show the partial pressures of the linear approximation p_1^{lin} and p_2^{lin}, while the solid line shows the total pressure of the non-linear approximation p^{nl} with initial decrease due to negative $\partial p^{\mathrm{nl}}/\partial N_2$

Then, the boundary $\hat{n}_1^{\mathrm{nl,\,bd}}(n_2)$ starts inside the non-linear domain, see App. A for details.

The reason for this behavior is the ratio of the amounts of small and large particles. There are much more small than large particles in the system for densities n_1, n_2 along the boundary $\hat{n}_1^{\mathrm{nl,\,bd}}(n_2)$ at high densities n_1: here, the fewer large particles are surrounded by many small particles. Therefore, the excluded volume interaction of the large particles in the non-linear pressure (16) is governed not by the simple term b_{11} but by the mixed term b_{12} which is distinctly smaller than b_{11} for $R_2 \ll R_1$. The maximum density achieved in the non-linear approximation $\max(\hat{n}_1^{\mathrm{nl}}) = 4/b_{11}$ is obtained for $R_2 \to 0$ and $N_2 \gg N_1$, i. e. these formulae go far beyond the traditional VdW results in the corresponding situation.

An example of pressure profiles for p_1^{lin}, p_2^{lin} and p^{nl} for $n_1 b_{11} = 0.9$ is shown in Fig. 1,*b*, where it is $R_2/R_1 = 0.4$ as in Fig. 1,*a*. The non-linear pressure (solid line) firstly decreases as the densities n_1, n_2 correspond to the region of negative partial derivatives, see Fig. 1,*a*. The partial pressures of the linear approximation are shown by dashed lines. The non-linear domain is seen to be larger, since it is one of the linear partial pressures which diverges first for increasing n_2.

We conclude that the linear and non-linear approximations show drastically different behaviors for high values of the large component's density n_1. In the linear approximation (19), the possible density values are below $1/b_{11}$ and $1/b_{22}$, respectively, and the derivatives $\partial p^{\mathrm{lin}}/\partial N_q$ are always positive. Whereas, in the non-linear approximation (16), higher densities $n_1 > 1/b_{11}$ are possible due to the occurence of negative derivatives $\partial p^{\mathrm{nl}}/\partial N_2 < 0$. This may be considered as pathological – or used as an advantage to describe special situations, e. g., densities $1/b_{11} < n_1 < \hat{n}_1^{\mathrm{nl}}$ for $R_2 \ll R_1$ (see App. A).

However, the use of any VdW approximation is in principle problematic for densities near $1/b_{qq}$. For low densities, the non-linear and linear approximations are practically equivalent, and the non-linear approximation is preferable, since the formulae are essentially simpler.

3. Grand Canonical Treatment

Since the number of particles is not conserved in relativistic statistical mechanics, it is more appropriate to use the grand canonical ensemble (GCE). The grand canonical partition function is built using the CPF,

$$\mathcal{Z}(T,V,\mu_1,\mu_2) =$$

$$= \sum_{N_1=0}^{\infty}\sum_{N_2=0}^{\infty} \exp\left[\tfrac{\mu_1 N_1+\mu_2 N_2}{T}\right] Z(T,V,N_1,N_2)\ , \qquad (24)$$

whereas the chemical potentials μ_1 and μ_2 correspond to components 1 and 2, respectively. The usual way to evaluate the GCE partition (24) to use the Laplace transform [20] or Laplace–Fourier transform [21] for infinite or finite systems, respectively. However, for the VdW CPF (14) or (18), one use the less complicated method by noting that there are limiting particle numbers $\hat{N}_1(N_2)$ or $\hat{N}_2(N_1)$, where each CPF becomes zero. For this reason, the above sum contains only a finite number of terms. Then it can be shown that, in the thermodynamical limit, (i. e. in the limit $V\to\infty$ for $N_q/V = \text{const}$) the grand canonical pressure $p(T,\mu_1,\mu_2) \equiv T\,\ln[\mathcal{Z}(T,V,\mu_1,\mu_2)]/V$ depends only on the maximum term of the double sum (24), where $N_1 = \mathcal{N}_1$ and $N_2 = \mathcal{N}_2$. One obtains

$$p(T,\mu_1,\mu_2) =$$

$$= \lim_{V\to\infty}\frac{T}{V}\,\ln\left[\exp\left[\tfrac{\mu_1\mathcal{N}_1+\mu_2\mathcal{N}_2}{T}\right] Z(T,V,\mathcal{N}_1,\mathcal{N}_2)\right]\ , \qquad (25)$$

wheras $\mathcal{N}_1$ and $\mathcal{N}_2$ are the average particle numbers.

3.1. Two VdW approximations

For the non-linear VdW approximation (14), the last expression takes the form

$$p^{\,\mathrm{nl}}(T,\mu_1,\mu_2) = \lim_{V\to\infty}\frac{T}{V}\,\ln\left[\tfrac{A_1^{\mathcal{N}_1}}{\mathcal{N}_1!}\,\tfrac{A_2^{\mathcal{N}_2}}{\mathcal{N}_2!}\,\times\right.$$

$$\left.\times\left(V-\mathcal{N}_1 b_{11}-\mathcal{N}_2 b_{22}+\tfrac{\mathcal{N}_1\mathcal{N}_2}{\mathcal{N}_1+\mathcal{N}_2}\,D\right)^{\mathcal{N}_1+\mathcal{N}_2}\right]\ , \qquad (26)$$

where $A_q = A(T,\mu_q;\ m_q,g_q) \equiv \exp[\mu_q/T]\,\phi_q$.

The evaluation of both maximum conditions for the grand canonical pressure

$$0 \stackrel{!}{=} \frac{\partial}{\partial\mathcal{N}_q}\left\{\ln\left[\tfrac{A_1^{\mathcal{N}_1}}{\mathcal{N}_1!}\,\tfrac{A_2^{\mathcal{N}_2}}{\mathcal{N}_2!}\,\times\right.\right.$$

$$\left.\left.\times\left(V-\mathcal{N}_1 b_{11}-\mathcal{N}_2 b_{22}+\tfrac{\mathcal{N}_1\mathcal{N}_2}{\mathcal{N}_1+\mathcal{N}_2}\,D\right)^{\mathcal{N}_1+\mathcal{N}_2}\right]\right\}\ , \qquad (27)$$

yields a system of two coupled transcendental equations,

$$\xi_1^{\mathrm{nl}}(T,\mu_1,\mu_2) =$$

$$= A_1\,\exp\left[-(\xi_1^{\mathrm{nl}}+\xi_2^{\mathrm{nl}})\,b_{11}+\tfrac{\xi_2^{\mathrm{nl}\,2}}{\xi_1^{\mathrm{nl}}+\xi_2^{\mathrm{nl}}}\,D\right], \qquad (28)$$

$$\xi_2^{\mathrm{nl}}(T,\mu_1,\mu_2) =$$

$$= A_2\,\exp\left[-(\xi_1^{\mathrm{nl}}+\xi_2^{\mathrm{nl}})\,b_{22}+\tfrac{\xi_1^{\mathrm{nl}\,2}}{\xi_1^{\mathrm{nl}}+\xi_2^{\mathrm{nl}}}\,D\right], \qquad (29)$$

where ξ_1^{nl} and ξ_2^{nl} are defined as

$$\xi_1^{\mathrm{nl}} \equiv \frac{\mathcal{N}_1}{V-\mathcal{N}_1 b_{11}-\mathcal{N}_2 b_{22}+\frac{\mathcal{N}_1\mathcal{N}_2}{\mathcal{N}_1+\mathcal{N}_2}\,D}\ , \qquad (30)$$

$$\xi_2^{\mathrm{nl}} \equiv \frac{\mathcal{N}_2}{V-\mathcal{N}_1 b_{11}-\mathcal{N}_2 b_{22}+\frac{\mathcal{N}_1\mathcal{N}_2}{\mathcal{N}_1+\mathcal{N}_2}\,D}\ . \qquad (31)$$

In the thermodynamical limit, the average particle numbers $\mathcal{N}_1$ and $\mathcal{N}_2$ are proportional to V as $\mathcal{N}_q = n_q^{\mathrm{nl}}\,V$. Then the volume V disappears in the definitions of ξ_1^{nl} and ξ_2^{nl} given by Eqs. (30) and (31), and they can be solved for either the density n_1^{nl} or n_2^{nl},

$$n_1^{\mathrm{nl}}(T,\mu_1,\mu_2) = \frac{\xi_1^{\mathrm{nl}}}{1+\xi_1^{\mathrm{nl}}b_{11}+\xi_2^{\mathrm{nl}}b_{22}-\frac{\xi_1^{\mathrm{nl}}\xi_2^{\mathrm{nl}}}{\xi_1^{\mathrm{nl}}+\xi_2^{\mathrm{nl}}}\,D}\ , \qquad (32)$$

$$n_2^{\mathrm{nl}}(T,\mu_1,\mu_2) = \frac{\xi_2^{\mathrm{nl}}}{1+\xi_1^{\mathrm{nl}}b_{11}+\xi_2^{\mathrm{nl}}b_{22}-\frac{\xi_1^{\mathrm{nl}}\xi_2^{\mathrm{nl}}}{\xi_1^{\mathrm{nl}}+\xi_2^{\mathrm{nl}}}\,D}\ . \qquad (33)$$

The $\xi_q^{\mathrm{nl}} = \xi_q^{\mathrm{nl}}(T,\mu_1,\mu_2)$ are the solutions of the coupled equations (28) and (29), respectively.

Hence, pressure (26) can be rewritten in terms of ξ_1^{nl} (28) and ξ_2^{nl} (29),

$$p^{\,\mathrm{nl}}(T,\mu_1,\mu_2) = T\,\left(\xi_1^{\mathrm{nl}}+\xi_2^{\mathrm{nl}}\right)\ , \qquad (34)$$

supposed that Eqs. (32) and (33) are taken into account. If definitions (30) and (31) are used for ξ_1^{nl} and ξ_2^{nl}, the pressure formula (34) coincides with the canonical expression (16) for $N_1 = \mathcal{N}_1$ and $N_2 = \mathcal{N}_2$.

Since the formulation is thermodynamically self-consistent, the identity $n_q \equiv \partial p(T,\mu_1,\mu_2)/\partial\mu_q$ leads to Eqs. (32) and (33) as well. The grand canonical formulae of the linear approximation [13] are obtained exactly as presented for the non-linear case in Eqs. (26)–(34). In the linear case, the two coupled transcendental equations are

$$\xi_1^{\mathrm{lin}}(T,\mu_1,\mu_2) = A_1\,\exp\left[-\xi_1^{\mathrm{lin}}\,b_{11}-\xi_2^{\mathrm{lin}}\,\tilde{b}_{12}\right]\ , \qquad (35)$$

$$\xi_2^{\mathrm{lin}}(T,\mu_1,\mu_2) = A_2\,\exp\left[-\xi_2^{\mathrm{lin}}\,b_{22}-\xi_1^{\mathrm{lin}}\,\tilde{b}_{21}\right]\ , \qquad (36)$$

with the definitions

$$\xi_1^{\rm lin} \equiv \frac{\mathcal{N}_1}{V - \mathcal{N}_1 b_{11} - \mathcal{N}_2 \tilde{b}_{21}} \ , \tag{37}$$

$$\xi_2^{\rm lin} \equiv \frac{\mathcal{N}_2}{V - \mathcal{N}_2 b_{22} - \mathcal{N}_1 \tilde{b}_{12}} \ . \tag{38}$$

The expressions for the particle densities are found by solving Eqs. (37) and (38) for either $n_1^{\rm lin}$ or $n_2^{\rm lin}$,

$$n_1^{\rm lin}(T,\mu_1,\mu_2) =$$

$$= \frac{\xi_1^{\rm lin}(1+\xi_2^{\rm lin}\,[b_{22}-\tilde{b}_{21}])}{1+\xi_1^{\rm lin}b_{11}+\xi_2^{\rm lin}b_{22}+\xi_1^{\rm lin}\xi_2^{\rm lin}\,[b_{11}b_{22}-\tilde{b}_{12}\tilde{b}_{21}]} \ , \tag{39}$$

$$n_2^{\rm lin}(T,\mu_1,\mu_2) =$$

$$= \frac{\xi_2^{\rm lin}(1+\xi_1^{\rm lin}\,[b_{11}-\tilde{b}_{12}])}{1+\xi_1^{\rm lin}b_{11}+\xi_2^{\rm lin}b_{22}+\xi_1^{\rm lin}\xi_2^{\rm lin}\,[b_{11}b_{22}-\tilde{b}_{12}\tilde{b}_{21}]} \ . \tag{40}$$

For the linear approximation, pressure (25) can be rewritten in terms of $\xi_1^{\rm lin}$ (35) and $\xi_2^{\rm lin}$ (36),

$$p^{\,\rm lin}(T,\mu_1,\mu_2) = T\,\left(\xi_1^{\rm lin}+\xi_2^{\rm lin}\right) \ , \tag{41}$$

if Eqs. (39) and (40) are taken into account, like in the non-linear case.

3.2. Comparison of both approximations

Let us briefly return to the usual VdW case, the one-component case. The corresponding transcendental equation is obtained from either Eqs. (28), (29) or (35), (36) by setting $R_1 = R_2 \equiv R$ and $A_1 = A_2 \equiv A$,

$$\xi^{\,\rm oc}(T,\mu) = A\,\exp\left[-\xi^{\,\rm oc}\,b\right] \ , \tag{42}$$

whereas $b \equiv b_{11} = b_{22}$. The transcendental factor $\exp[-\xi^{\,\rm oc}\,b]$ has the form of a suppression term, and the solution $\xi^{\,\rm oc} \equiv p^{\,\rm oc}/T$ of this transcendental equation evidently decreases with increasing b for constant T and μ. Then, in turn, the corresponding particle density $n^{\,\rm oc} = \xi^{\,\rm oc}/(1+\xi^{\,\rm oc}\,b)$ is suppressed in comparison with that of the ideal gas due to the lower $\xi^{\,\rm oc}$ and the additional denominator. Thus, the suppressive transcendental factor corresponds to the suppression of particle densities.

Now it can be seen from Eqs. (28), (29) and (35), (36) that the transcendental factors of both two-component approximations contain as well this usual one-component- or VdW-like suppressive part $\exp[-(p/T)\,b_{qq}]$. But since $D \geq 0$ and $\tilde{b}_{pq} < b_{pp}$, respectively, there is furthermore the attractive part in each corresponding transcendental factor.

In a non-linear approximation, the attractive part can even dominate the suppressive part for the smaller component, e.g., in Eq. (29) for $R_2 < R_1$. Then the larger component can reach densities $n_1^{\rm nl}$ higher than $1/b_{11}$ analogous to the CE. A detailed discussion is given in App. C.

High densities in the canonical treatment correspond to large values of the chemical potentials in the grand canonical treatment. In the limit

$$\mu_1/T \to \infty \ \ (T,\mu_2 = \text{const.}) \quad \text{or} \quad \xi_1^{\rm nl} \to \infty, \tag{43}$$

the solution of Eq. (29), $\xi_2^{\rm nl}$, can be enhanced for increasing $\xi_1^{\rm nl}$ instead of being suppressed, if R_2 is sufficiently small. This may be called the non-linear enhancement. The behavior of the non-linear approximation in limit (43) depends only on the ratio of two radii R_1/R_2 and is characterized by the coefficient

$$a_2 \equiv \sqrt{D/b_{22}} - 1 \ . \tag{44}$$

A negative a_2 is related to the suppressive transcendental factor in Eq. (29). For equal radii $R_2 = R_1$, $a_2 = -1$, and the suppression is evidently not reduced but VdW-like. For $-1 < a_2 < 0$, this suppression is reduced, the most strongly for $a_2 \approx 0$.

In the case $a_2 = 0$, the suppression for $\xi_2^{\rm nl}$ (29) disappears in limit (43), and one has $\xi_2^{\rm nl} \to A_2 = \text{const}$. This case provides the critical radius $R_{2,\,\rm crit}$ (23).

For $a_2 > 0$ or $R_2 < R_{2,\,\rm crit}$, the non-linear enhancement of $\xi_2^{\rm nl}$ occurs for increasing $\xi_1^{\rm nl}$; it is the stronger the larger is a_2. Then $n_1^{\rm nl}$ (32) can exceed $\max(n_1^{\rm oc}) = 1/b_{11}$, whereas $n_2^{\rm nl}$ (33) does not vanish (see App. C for the explicit fomulae). The density $\max(\hat{n}_1^{\rm nl}) = 4/b_{11}$ is achieved for $a_2 \to \infty$ or $R_2 \to 0$.

The suppression in the transcendental factor of $\xi_1^{\rm nl}$ (28) is generally reduced for $R_2 < R_1$, the more strongly the smaller R_2 is, but there is no enhancement possible in limit (43).

4. Relativistic Excluded Volumes

In this section, we will investigate the influence of relativistic effects on the excluded volumes of fast moving particles by accounting for their ellipsoidal shape due to the Lorentz contraction. In [18], a quite simple ultra-relativistic approach has been made to estimate these effects: instead of ellipsoids, two cylinders with the corresponding radii have been used to calculate approximately the excluded volume term b_{pq} for a two-component mixture. The resulting relativistic excluded volumes depend on the temperature and contain the

radii and the masses as parameters. The simple non-mixed term reads [14]

$$b_{qq}(T) = \alpha_{qq} \left(\frac{37\pi}{9} \frac{\sigma_q}{\phi_q} + \frac{\pi^2}{2} \right) R_q^3 \ , \tag{45}$$

where $\sigma_q \equiv \sigma(T; m_q, g_q)$ denotes the ideal gas scalar density,

$$\sigma(T; m, g) = \frac{g}{2\pi^2} \int\limits_0^\infty \mathrm{d}k \, k^2 \, \frac{m}{E(k)} \, \exp\left[-\tfrac{E(k)}{T} \right] \ . \tag{46}$$

The expression for the mixed case can be derived similarly from [18],

$$b_{12}(T) = \alpha_{12} \left\{ \left(\tfrac{\sigma_1}{\phi_1} \, f_1 + \tfrac{\pi^2}{4} \tfrac{R_2}{R_1} \right) R_1^3 + \right.$$

$$\left. + \left(\tfrac{\sigma_2}{\phi_2} \, f_2 + \tfrac{\pi^2}{4} \tfrac{R_1}{R_2} \right) R_2^3 \right\} \ , \tag{47}$$

whereas the abbreviations f_1 and f_2 are dimensionless functions of both radii,

$$f_1 = \tfrac{\pi}{3} \left(2 + \tfrac{3R_2}{R_1} + \tfrac{7R_2^2}{6R_1^2} \right) \ , \qquad f_2 = \tfrac{\pi}{3} \left(2 + \tfrac{3R_1}{R_2} + \tfrac{7R_1^2}{6R_2^2} \right) \ .$$

The normalization factors

$$\alpha_{11} = \alpha_{22} = \frac{16}{\frac{37}{3} + \frac{3\pi}{2}} \ , \tag{48}$$

$$\alpha_{12} = \frac{\frac{2\pi}{3}(R_1+R_2)^3}{f_1 + \frac{\pi^2}{4}\frac{R_2}{R_1} \quad R_1^3 + \quad f_2 + \frac{\pi^2}{4}\frac{R_1}{R_2} \quad R_2^3} \tag{49}$$

are introduced to normalize the ultra-relativistic approximations (45) and (47) for $T = 0$ to the corresponding non-relativistic results. For the hadron gas, however, these Boltzmann statistical formulae will only be used at high temperatures, where effects of quantum statistics are negligible.

Note that it is not appropriate to consider temperature dependent hard-core radii $R_p(T)$ or $R_q(T)$, since the $b_{pq}(T)$ terms give the Lorentz-contracted excluded volumes and are involved functions of T, m_p, m_q, R_p and R_q. However, for a given value of $b_{pq}(T)$, the necessary hard-core radii R_p and R_q will obviously depend on the temperature.

It is evident that formulae (45) and (47) suffice already for the multicomponent case, because even a multicomponent VdW formulation contains only b_{pq} terms.

For both approximations, the expressions for pressure (34) or (41) and the corresponding particle densities (32) and (33) or (39) and 40) remain unchanged. However, due to the temperature dependence of the relativistic excluded volumes, the entropy density is modified:

$$s(T, \mu_1, \mu_2) \equiv \frac{\partial}{\partial T} \, p(T, \mu_1, \mu_2) \equiv$$

$$\equiv s_{\mathrm{nrel}} + s_{\mathrm{rel}}(\partial_T b_{11}, \partial_T b_{22}, \partial_T b_{12}) \ . \tag{50}$$

The additional term s_{rel} depends on the temperature derivatives of relativistic excluded volumes, $\partial_T b_{pq} \equiv \partial b_{pq}/\partial T$, which represent their thermal compressibility.

Furthermore, the term s_{rel} generates additional terms for the energy density, according to $e \equiv Ts - p + \mu_1 n_1 + \mu_2 n_2$. In the non-linear approximation, one obtains

$$e^{\,\mathrm{nl}}(T, \mu_1, \mu_2) = n_1^{\mathrm{nl}} \, \frac{\epsilon_1}{\phi_1} + n_2^{\mathrm{nl}} \, \frac{\epsilon_2}{\phi_2} - (n_1^{\mathrm{nl}} + n_2^{\mathrm{nl}}) \, T^2 \times$$

$$\times \left(\xi_1^{\mathrm{nl}} \, \partial_T b_{11} + \xi_2^{\mathrm{nl}} \, \partial_T b_{22} - \tfrac{\xi_1^{\mathrm{nl}} \, \xi_2^{\mathrm{nl}}}{\xi_1^{\mathrm{nl}} + \xi_2^{\mathrm{nl}}} \, \partial_T D \right) \ , \tag{51}$$

and the linear approximation yields

$$e^{\,\mathrm{lin}}(T, \mu_1, \mu_2) = n_1^{\mathrm{lin}} \, \frac{\epsilon_1}{\phi_1} + n_2^{\mathrm{lin}} \, \frac{\epsilon_2}{\phi_2} -$$

$$- n_1^{\mathrm{lin}} \, T^2 \left(\xi_1^{\mathrm{lin}} \, \partial_T b_{11} + \xi_2^{\mathrm{lin}} \, \partial_T \tilde{b}_{12} \right) -$$

$$- n_2^{\mathrm{lin}} \, T^2 \left(\xi_2^{\mathrm{lin}} \, \partial_T b_{22} + \xi_1^{\mathrm{lin}} \, \partial_T \tilde{b}_{21} \right) \ , \tag{52}$$

whereas $\epsilon_q \equiv \epsilon(T; m_q, g_q)$ denotes the ideal gas energy density

$$\epsilon(T; m, g) = \frac{g}{2\pi^2} \int\limits_0^\infty \mathrm{d}k \, k^2 \, E(k) \, \exp\left[-\tfrac{E(k)}{T} \right] \ . \tag{53}$$

The additional terms in the entropy density (50) and in the energy density (51) or (52) which contain the temperature derivatives do evidently not occur in the case of the usual non-relativistic, i.e. constant, excluded volumes.

Let us now study the hadronic equation of state generated by each of the two-component VdW approximations and their modifications due to relativistic excluded volumes. When used to describe hadronic particles, the hard-core radii R_q should be considered as parameters rather than particle radii. We identify the first component as nucleons ($m_1 \equiv m_{\mathrm{n}} = 939$ MeV, $\mu_1 \equiv \mu_{\mathrm{n}} = \mu_{\mathrm{B}}$ and $g_1 \equiv g_{\mathrm{n}} = 4$ for symmetric nuclear matter) and the second as pions ($m_2 \equiv \overline{m}_\pi = 138$ MeV, $\mu_2 \equiv \mu_\pi = 0$ and $g_2 \equiv g_\pi = 3$). Quantum statistical effects other than the degeneracy factors g_q are neglected. To reproduce experimental data, however,

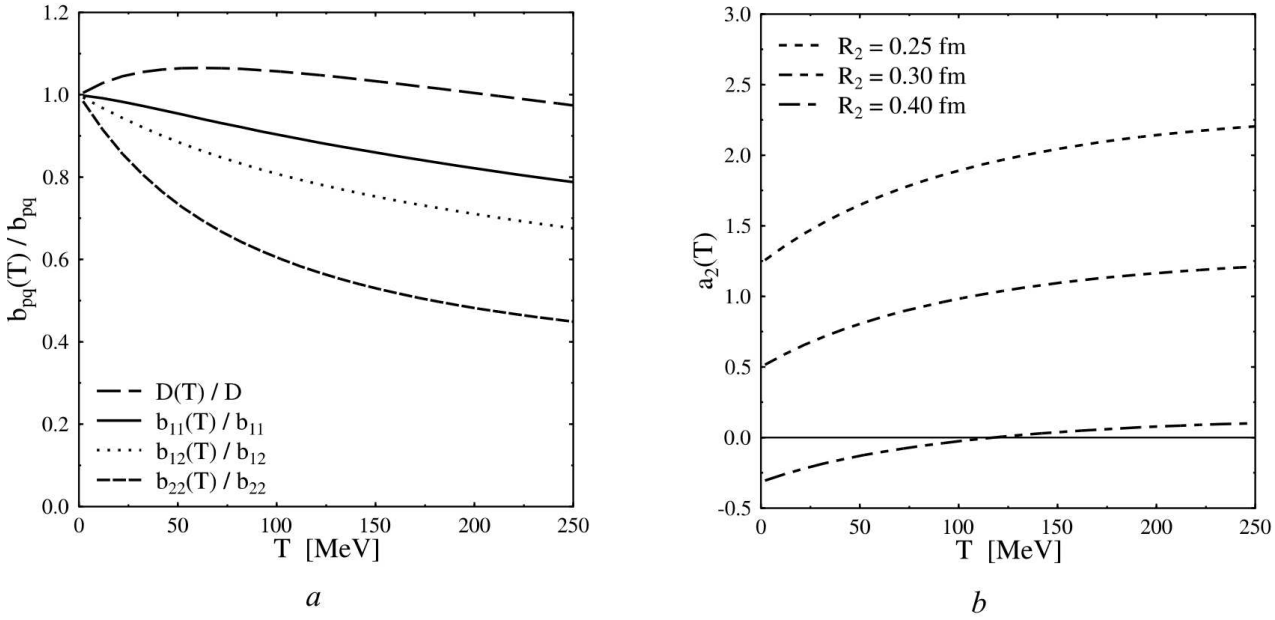

Fig. 2. Temperature dependence of the relativistic excluded volume terms for $m_1 = m_\mathrm{n}, m_2 = \overline{m}_\pi, R_1 = 0.6$ fm. *a* – relative values for $R_2 = 0.3$ fm: $b_{11}(T)/b_{11}$, $b_{12}(T)/b_{12}$, $b_{22}(T)/b_{22}$ and $D(T)/D$ (solid line, dotted line, short and long dashes, respectively). The relativistic excluded volume of light species ($b_{22}(T)/b_{22}$) is affected more strongly by temperature. *b* – the characteristic coefficient of the non-linear approximation $a_2(T) = (\sqrt{D(T)/b_{22}(T)} - 1)$ for various $R_2 = 0.25$, 0.3, and 0.4 fm. The non-linear enhancement ($a_2(T) > 0$) becomes stronger due to a decrease of the relativistic excluded volumes with increase in the temperature

it would be necessary to consider all hadrons and hadronic resonances as well as the contributions from hadronic decays into daughter hadrons.

For some examples, the temperature dependence of the relativistic excluded volumes is shown in Fig. 2,*a*, given in units of the corresponding non-relativistic terms, $b_{pq} = b_{pq}(0)$. The solid line and the short dashes show the basic excluded volumes $b_{11}(T)$ and $b_{22}(T)$, respectively. In these relative units, the decreases of $b_{11}(T)$ and $b_{22}(T)$ depend only on the corresponding masses. It is apparent that the pion excluded volume $b_{22}(T)$ is affected much stronger than the excluded volume of nucleons, $b_{11}(T)$. The dotted line shows the mixed volume term $b_{12}(T)$, and the long dashes show the compound volume term $D(T) \equiv b_{11}(T) + b_{22}(T) - 2b_{12}(T)$. These two terms depend obviously on both masses and both radii.

The curves for the generalized excluded volume terms of the linear approximation $\tilde{b}_{12}(T)$ and $\tilde{b}_{21}(T)$ behave similarly to $b_{12}(T)$.

Introducing the relativistic excluded volumes $b_{pq}(T)$, however, has two effects. First, the maximum densities become larger, since $1/b_{qq}(T) > 1/b_{qq}$ generally, as seen in Fig. 2,*a*. Furthermore, the balance between the lighter and the heavier species is changed because the lighter species is affected more than the heavier ones at the same temperature. For the above parameters, $b_{22}(T)/b_{22} \leq b_{11}(T)/b_{11}$.

In the non-linear approximation, this balance is characterized by the coefficient a_2 defined by Eq. (44). In Fig. 2,*b* the temperature dependence of $a_2(T) \equiv (\sqrt{D(T)/b_{22}(T)} - 1)$ is shown for three different values of R_2. The relativistic coefficient $a_2(T)$ increases with T, i. e. the non-linear enhancement becomes stronger for higher temperatures. For some values of R_2, e. g., $R_2 = 0.4$ fm, a primary suppression $a_2(0) \equiv a_2 < 0$, turns into an enhancement $a_2(T) > 0$, when the temperature is sufficiently high. For temperature dependent excluded volumes, $R_{2,\,\mathrm{crit}}$ looses its meaning; here, only $a_2(T) > 0$ is the valid condition for the occurrence of the non-linear enhancement or densities $n_1^{\mathrm{nl}} > 1/b_{11}(T)$.

The linear coefficient, $\tilde{a}_2(T) = -2b_{12}(T)/(b_{11}(T) + b_{22}(T))$, is not strongly affected by the temperature for the above choice of hadronic parameters: it increases slightly with T but remains negative. Hence, changes in the balance between the lighter and the heavier species play a minor role for the linear approximation.

Particle densities for nucleons and pions in units of $n_0 = 0.16$ fm^{-3} vs. $\mu_1/m_1 \equiv \mu_\mathrm{n}/m_\mathrm{n}$ are shown in

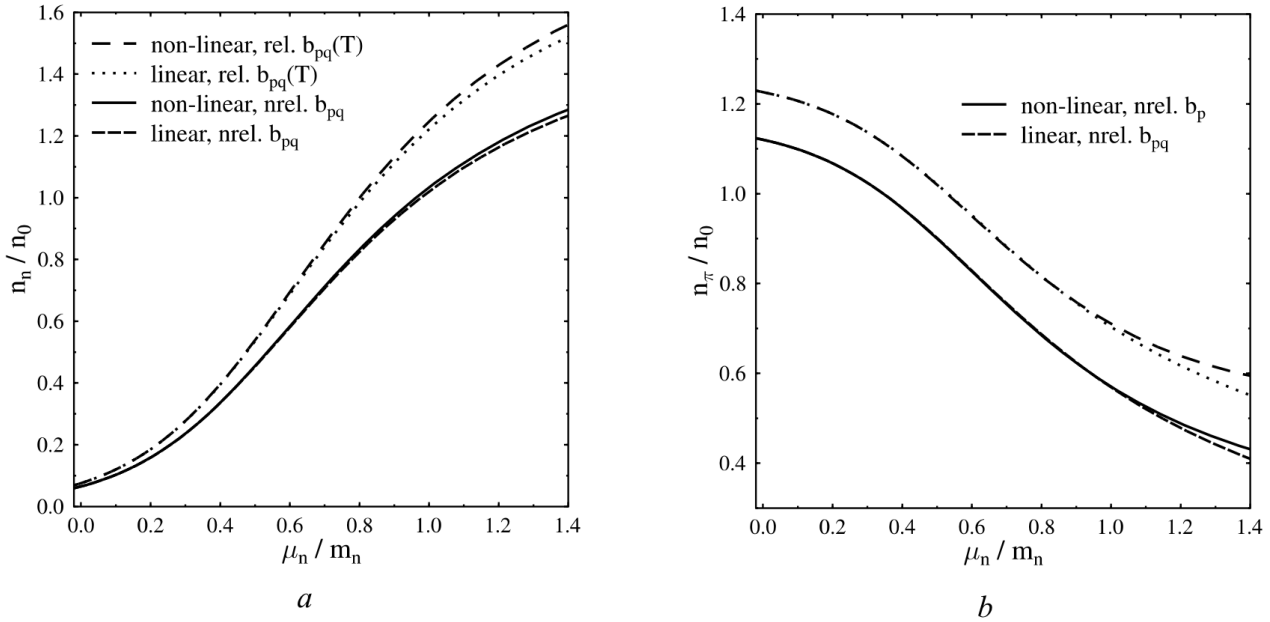

Fig. 3. Comparison of the model predictions for the nucleon (a) and pion (b) densities $n_{\rm n}$ and n_π, respectively, vs $\mu_{\rm n}/m_{\rm n}$ ($R_1 = 0.6$ fm, $R_2 = 0.3$ fm and $T = 185$ MeV, densities in units of $n_0 = 0.16$ fm^{-3}). In both figures, two upper lines correspond to relativistic excluded volumes $b_{pq}(T)$ and two lower lines to non-relativistic excluded volumes b_{pq}. The results of the linear and non-linear approximations coincide – only for extremely large $\mu_{\rm n}/m_{\rm n}$, the non-linear results lie slightly higher than the corresponding linear results. The deviations due to relativistic excluded volumes are significant

Figs. 3,a and b for $T = 185$ MeV. The linear and non-linear results are shown for constant excluded volumes with short dashes and solid lines, respectively, and further, for relativistic excluded volumes, with dotted lines and long dashes, respectively. At this high temperature, the relativistic results are significantly higher than the non-relativistic one. A difference between the linear and non-linear approximations due to the non-linear enhancement becomes noticeable only for high $\mu_{\rm n}/m_{\rm n} > 0.8$. Thus, for $R_{\rm n} = R_1 = 0.6$ fm from above, the linear and non-linear approximations are practically equivalent for nucleon densities below $n_{\rm n} \approx 0.8\, n_0$, i. e. for densities below about $n_1 \approx 1/(2\, b_{11})$. On the other hand, due to the strong decrease of $b_{22}(T)$ with increase in the temperature, the influence of the relativistic excluded volumes is essential for temperatures of the order of $T \approx m_\pi$.

The presence of the additional terms containing the temperature derivatives in the energy density (51) or (52) makes it impossible to convert a VdW gas with relativistic excluded volumes into a gas of free streaming particles. Therefore, it is problematic to use these formulae for the post-freeze-out stage. For the latter, the quantities of free streaming particles without any interaction should be used, see the discussion in [22,23] and references therein. However, these equations of state may be used to describe the stage between chemical and thermal freeze-outs, i.e. the pre-freeze-out stage in terms of [22,23]. This is examplified in the next section.

5. Hard-core Radii from Particle Yield Ratios

As a simple application of the above-presented equations of state, let us re-evaluate the thermal model fit parameters for particle yield ratios of [6], namely the hard-core radii of pions R_π and other hadrons R_0. A two-component VdW excluded volume model has been used there to explain the pion abundance in (A+A)-collisions by a smaller hard-core radius for pions than that for the other hadrons. The ratios has been fitted to BNL AGS (Au+Au at 11 A GeV) and CERN SPS (Pb+Pb at 160 A GeV) data [7] within a thermal model, including all resonances up to 2 GeV and using quantum statistics.

The applied model, however, corresponds to the incorrect separated model as pointed out in Sect. 1. For convenience, we give these formulae in the Boltzmann approximation. Within the previously defined notation,

the two coupled transcendental equations read

$$\xi_1^{\rm sp}(T,\mu_1,\mu_2) = A_1\,\exp\left[-(\xi_1^{\rm sp}+\xi_2^{\rm sp})\,b_{11}\right]\ , \tag{54}$$

$$\xi_2^{\rm sp}(T,\mu_1,\mu_2) = A_2\,\exp\left[-(\xi_1^{\rm sp}+\xi_2^{\rm sp})\,b_{22}\right]\ , \tag{55}$$

wheras $p^{\rm sp}(T,\mu_1,\mu_2) = T\,(\xi_1^{\rm sp}+\xi_2^{\rm sp})$. In this context, A_1 represents a sum over the contributions of all hadron species but pions, while A_2 corresponds to pions only.

The expressions for the particle densities are obtained from $n_q^{\rm sp} \equiv \partial p^{\rm sp}/\partial\mu_q$,

$$n_1^{\rm sp}(T,\mu_1,\mu_2) = \frac{\xi_1^{\rm sp}}{1+\xi_1^{\rm sp}b_{11}+\xi_2^{\rm sp}b_{22}}\ , \tag{56}$$

$$n_2^{\rm sp}(T,\mu_1,\mu_2) = \frac{\xi_2^{\rm sp}}{1+\xi_1^{\rm sp}b_{11}+\xi_2^{\rm sp}b_{22}}\ . \tag{57}$$

Solving these equations for $\xi_1^{\rm sp}$ and $\xi_2^{\rm sp}$, one recovers the canonical pressure formula of the separated model (11) as announced in Sect. 2.

Due to the separation of both components in this model, there is no excluded volume term b_{12} for the interaction between different components at all. This is an essential difference to both the linear and non-linear approximations. Note that the separated model is not a two-component VdW approximation because it cannot be obtained by approximating the CPF (13).

The transcendental factors of formulae (54) and (55) exhibit a constant VdW-like suppression $\exp[-(p/T)\,b_{qq}]$. There is a reduction of this suppression in the linear and non-linear approximations, as discussed in Sect. 3. The VdW-like suppression is reduced, if b_{12} appears in the corresponding formulae since b_{12} is smaller than b_{11} for $R_2 < R_1$. It is evident that the deviation of the linear and non-linear approximationa from the separated model is the larger, the more R_1 and R_2 differ from each other.

In the first step of the fit procedure of [6], only the hadron ratios excluding pions have been taken to find the freeze-out parameters. $T \approx 140$ MeV, $\mu_{\rm B} \approx 590$ MeV for AGS and $T \approx 185$ MeV, $\mu_{\rm B} \approx 270$ MeV for SPS have been obtained. In the second step, a parameter introduced as the pion effective chemical potential μ_π^* has been fitted to the pion-to-hadron ratios. Using the Boltzmann statistics, it can be shown that the pion enhancement is thoroughly regulated by the value of μ_π^* [6]; one has obtained $\mu_\pi^* \approx 100$ MeV for AGS and $\mu_\pi^* \approx 180$ MeV for SPS data, respectively.

The pion effective chemical potential depends explicitly on the excluded volumes but also on the pressure. The pressure itself is a transcendental function depending solely on the excluded volumes, since T and $\mu_{\rm B}$ are already fixed by step one. In [6], the formula $\mu_\pi^* \equiv (v_0 - v_\pi)\,p(v_0,v_\pi)$ has been obtained for the separated model, where $v_\pi \equiv b_{22}$ and $v_0 \equiv b_{11}$ are the excluded volumes corresponding to the hard-core radii of pions $R_\pi \equiv R_2$ and other hadrons $R_0 \equiv R_1$, respectively. Thus, the μ_π^* values for AGS and SPS data define two curves in the R_π–R_0-plane. The main conclusion of [6] is that the intersection point of these two curves ($R_\pi = 0.62$ fm, $R_0 = 0.8$ fm) gives the correct pair of hard-core radii for pions and for the other hadrons, i. e. the AGS and SPS data are fitted simultaneously within the applied model.

In [8], these values of R_0 and R_π have been criticized for being unreasonably large. There, a complete fit of solely SPS data has been performed within a separated model. The best fit has been obtained for equal hard-core radii, $R_\pi = R_0 = 0.3$ fm, motivated by nucleon scattering data. Good agreement has been found as well for a baryon hard-core radius, $R_{\rm Bar} = 0.3$ fm, and a common hard-core radius for all mesons, $R_{\rm Mes} = 0.25$ fm, choosen in accord with the above ratio of radii, $R_0/R_\pi = 0.8/0.62$. Larger hard-core radii, especially those of [6], are quoted as giving a distinctly worse agreement.

Assuming the validity of the Boltzmann statistics, we have re-calculated the $R_0(R_\pi)$-curves for the above μ_π^* values; firstly in the separated model (54)–(57), i. e. as presented in [6]. The resulting curves shown as thin lines in Fig. 4,*a* naturally match the results of the underlying fit of [6] which are indicated by markers.

Then we have considered the linear and non-linear approximations. Due to the occurence of b_{12} terms in these two cases, both functional forms of μ_π^* are essentially different from those in the separated case. Consequently, the shapes of the $R_0(R_\pi)$-curves are different as well. We find distinct deviations from the separated model, especially for $R_\pi \to 0$, and the values for the intersection point are slightly lower; see thin lines in Fig. 4,*b* for the linear exrapolation. The non-linear approximation gives identical results for this purpose because the hadron densities are too small for a noticeable non-linear enhancement.

The crucial point is now to turn on the relativistic temperature dependence of the excluded volumes. To keep the analysis simple, we treat only pions this way since they give the strongest effect.

Although the other hadrons are assumed to have equal hard-core radii, their relativistic excluded volumes would be different for $T > 0$, according to their different masses. To check the influence of relativistic excluded volumes for all particles, we have used one average mass

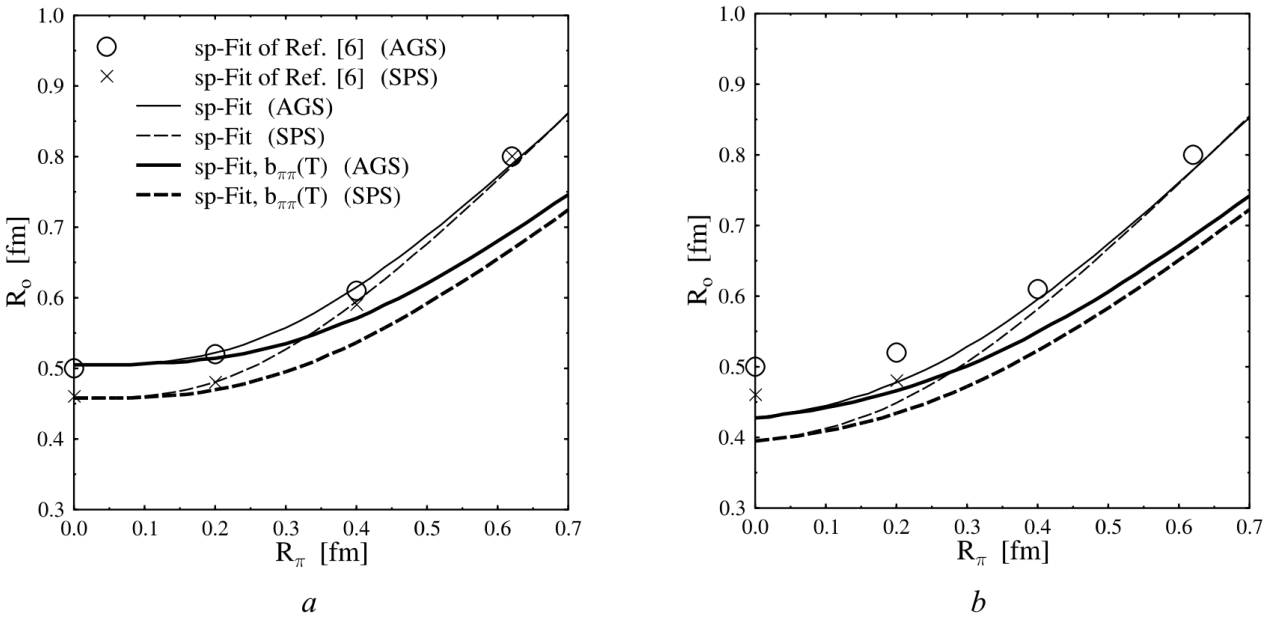

Fig. 4. Fits of particle yield ratios for the AGS and SPS data [7] with the separated model and the linear approximation. The thin lines show the fits for the separated model (a) and the linear approximation (b); the non-linear approximation gives identical results for the latter case. The thick lines in (a) and (b) show the corresponding curves for relativistic excluded volumes $v_\pi = b_{22}(T)$: there is no intersection for either of the three models. In both plots, the results of the fit from [6] for the AGS and SPS data are indicated by circles and crosses, respectively

of 1 GeV for all other hadrons. The corresponding change in the R_0-values are below 5%.

The results of the fit for relativistic excluded volumes for pions are shown in Figs. 4,a and b as thick lines. Though this approach is more realistic, there is no intersection point for any of the three models even for very large radii $R_0, R_\pi \gg 0.5$ fm. For the approximated case of a single averaged hadron mass, there is no intersection either. Because of the different freeze-out temperatures for AGS and SPS, the $v_\pi(T) \equiv b_{22}(T)$ values are changed differently in both cases, and so are the scales for the corresponding R_π.

Due to the errors in experimental data, one ought to obtain a corridor instead of a curve for each set of data. Consequently, the particle yield ratios can be reproduced well by e. g., $R_0 \approx 0.4$ fm, $R_\pi \approx 0.2$ fm or larger values for any of the models with relativistic excluded volumes. Therefore, we conclude that the fit procedure proposed in [6] is not suitable to find a unique pair of hard-core radii for pions and other hadrons, as long as a best fit is searched for just two sets of the data on particle yield ratios. The use of a relativistic excluded volume for pions along with a correct approximation reduce the value of the necessary nucleon hard-core radius essentially towards more realistic values.

6. Summary

In the present work, several equations of state for the two-component van der Waals excluded volume model are derived and investigated. We have discussed two essentially different formulations, the linear and non-linear approximations.

The non-linear approximation is the simplest possibility. Here, the large component can reach higher densities n_1 than the usual limiting VdW density $1/b_{11}$, if the other component has a suffiently small hard-core radius, $R_2 < R_{2,\,\mathrm{crit}}$. In the linear approximation, the densities cannot exceed the usual limiting VdW densities $1/b_{11}$ and $1/b_{22}$, but generalized excluded volume terms have to be introduced.

For both approximations, the suppression factors of the grand canonical formulae contain a VdW-like term proportional to $\exp[-(p/T)\, b_{qq}]$ which is reduced non-trivially, however. In the linear case, there is a slight reduction, whereas this reduction can turn the suppression even into an enhancement for the smaller component in the non-linear case, which leads to the exceeding of $1/b_{11}$ for the density of the larger component n_1.

The commonly used formulae of the separated model are shown to be not suitable for the two-component case, because they correspond to a system, where both components are separated from each other and cannot mix. In this model, the grand canonical suppression factor is just VdW-like and has no reduction of the suppression.

Furthermore, relativistic, i.e. Lorentz-contracted, excluded volumes have been introduced. Naturally, the relativistic excluded volume per particle decreases with increase in the temperature. This effect is the stronger, the lighter the particle species is. The suppression of the particle densities in VdW models is lower for a component of smaller excluded volume in comparison with a component of larger excluded volume. Therefore, the temperature dependence of the relativistic excluded volumes causes a reduction of the suppression of particle densities.

The full equations of state have been presented, for both the linear and non-linear approximations, with constant and with relativistic excluded volumes. For the entropy density and the energy density, there are additional terms containing the temperature derivatives of the relativistic excluded volume terms due to their 'thermal compressibility'. In comparison with the non-relativistic case, the expressions for the pressure and the particle densities remain unchanged, but the possible range of values is obviously wider, since, generally, $1/b_{11}(T) \geq 1/b_{11}$ and $1/b_{22}(T) \geq 1/b_{22}$.

As an application of the derived formulations, a fit of particle yield ratios for SPS and AGS has been re-evaluated. In [6], this fit had been done in the separated model by adjusting the hard-core radii for pions R_π and for other hadrons R_0. The results of the new fit are essentially different from those in the separated model but coincide for both the linear and non-linear approximations. The picture changes drastically, however, if relativistic excluded volumes are adopted for pions. The basic idea of the fit – one pair of hard-core radii suffices to fit the AGS and SPS data simultaneously – does not lead to a result anymore. This is the case for the separated model and for both approximations, linear and non-linear. Experimental uncertainties lead to a region of possible values in the R_0–R_π-plane; one could describe the data for $R_\mathrm{o} \geq 0.4$ fm and $R_\pi \geq 0.2$ fm.

We conclude that there are two causes of an enhancement of particle densities, e.g., the thermal pion abundance, in VdW descriptions: First, the density suppression is generally lower for the smaller component in two-component models. Second, there is a further reduction of the density suppression due to the relativistic excluded volumes. The latter are essentially smaller for light hadron species than for heavy species, especially for temperatures $T \gg 50$ MeV.

When applied to the hadron gas, the linear and non-linear results almost coincide for nucleon densities up to $n_0 \approx 0.16$ fm^{-3} (for $R_0 \leq 0.6$ fm), since the non-linear enhancement does not appear there, but the deviation from the incorrect separated model is distinct. However, the formulae of the non-linear approximation are essentially simpler than these of the linear approximation.

The influence of relativistic effects on the excluded volumes becomes indispensable for the temperatures typical of heavy ion collisions. Therefore, it is necessary to include a correct two- or multicomponent VdW approximation – linear or non-linear – as well as relativistic excluded volumes in future calculations.

The authors thank D.H. Rischke for useful discussions and St. Hofmann for valuable comments. The research made in this work was supported in part by the Program "Fundamental Properties of Physical Systems under Extreme Conditions" of the Bureau of the Division of Physics and Astronomy of the National Academy of Science of Ukraine.

APPENDIX A: Two VdW Approximations in the CE

In what follows, we will study the differences between the linear and non-linear approximations: the total excluded volumes $v_q = v_q(N_1, N_2)$ of the corresponding partial pressures. In the linear pressure formula (19), each component has its own total excluded volume given by

$$v_1^{\mathrm{lin}} \equiv N_1 b_{11} + N_2 \tilde{b}_{21} \ , \quad v_2^{\mathrm{lin}} \equiv N_1 \tilde{b}_{12} + N_2 b_{22} \ , \tag{58}$$

whereas, in the non-linear pressure formula (16), there is the common total excluded volume for both components

$$v_1^{\mathrm{nl}} = v_2^{\mathrm{nl}} = v^{\,\mathrm{nl}} \equiv N_1 b_{11} + N_2 b_{22} - \tfrac{N_1 N_2}{N_1+N_2} D \ . \tag{59}$$

It can be readily checked that it is either $v_1^{\mathrm{lin}} \leq v^{\,\mathrm{nl}} \leq v_2^{\mathrm{lin}}$ or $v_1^{\mathrm{lin}} \geq v^{\,\mathrm{nl}} \geq v_2^{\mathrm{lin}}$, i.e. the pole corresponding to the non-linear pressure always lies between both poles corresponding to the linear pressure. Hence, there are values N_1, N_2, where the non-linear pressure is still finite, but the linear pressure formula is yet invalid since one of the partial pressures has already become infinite. Consequently, the domain of the non-linear approximation is larger.

For given V, the two domains can be expressed by the limiting densities (21) and (22), which are defined by the poles $v_q(N_1, N_2) = V$ for the corresponding pressure. In the linear approximation, one obtains the expressions

$$\hat{n}_{1,1}^{\mathrm{lin}}(n_2) = \frac{1 - \tilde{b}_{21} n_2}{b_{11}} \ , \qquad \hat{n}_{1,2}^{\mathrm{lin}}(n_2) = \frac{1 - b_{22} n_2}{\tilde{b}_{12}} \ . \tag{60}$$

For given n_2, therefore, the domain of $p^{\,\mathrm{lin}}$ (19) is

$$0 \leq n_1^{\mathrm{lin}} < \min\left\{ \hat{n}_{1,1}^{\mathrm{lin}}(n_2),\ \hat{n}_{1,2}^{\mathrm{lin}}(n_2) \right\} \ . \tag{61}$$

In the non-linear approximation, there is solely one limiting density

$$\hat{n}_1^{\,\mathrm{nl}}(n_2) = \frac{1-2\,b_{12}n_2+\sqrt{(1-2b_{12}n_2)^2+4b_{11}n_2\,(1-b_{22}n_2)}}{2\,b_{11}} \quad . \tag{62}$$

Consequently, for given n_2, the domain of $p^{\,\mathrm{nl}}$ (16) is

$$0 \le n_1^{\,\mathrm{nl}} < \hat{n}_1^{\,\mathrm{nl}}(n_2) \; . \tag{63}$$

In the non-linear approximation, there is furthermore a region, where the pressure has negative partial derivatives with respect to the smaller particles' number, $\partial p^{\,\mathrm{nl}}/\partial N_2 < 0$. The condition $\partial p^{\,\mathrm{nl}}/\partial N_2 = 0$ defines the boundary of this region

$$\hat{n}_1^{\,\mathrm{nl,\,bd}}(n_2) =$$

$$= \frac{1-2\,(b_{12}-b_{22})\,n_2+\sqrt{(1-2\,(b_{12}-b_{22})\,n_2)^2+8\,(b_{11}-b_{12})\,n_2}}{4\,(b_{11}-b_{12})} \quad . \tag{64}$$

For given n_2, a negative derivative $\partial p^{\,\mathrm{nl}}/\partial N_2 < 0$ occurs only at a density $n_1 > \hat{n}_1^{\,\mathrm{nl,\,bd}}$, while the derivative $\partial p^{\,\mathrm{nl}}/\partial N_1$ is always positive for $R_2 \le R_1$, as readily checked.

In Fig. 1,*a*, the functions $\hat{n}_1(n_2)$ are presented in dimensionless variables $\hat{n}_1 b_{11}$ and $n_2 b_{22}$. The properties of these dimensionless functions depend only on the ratio of two radii R_2/R_1. The smaller this ratio is, the higher is the maximum value of $\hat{n}_1^{\,\mathrm{nl}}$, while the region of negative derivatives $\partial p^{\,\mathrm{nl}}/\partial N_2$ becomes narrower. The straight line $\hat{n}_{1,1}^{\,\mathrm{lin}}(n_2)$ starts always at $1/b_{11}$, but its slope decreases for smaller R_2/R_1, whereas $\hat{n}_{1,2}^{\,\mathrm{lin}}(n_2)$ ends at $1/b_{22}$ and its slope increases. The pressure of the separated model (11) would yield one straight line from $n_1 b_{11} = 1$ to $n_2 b_{22} = 1$ in Fig. 1,*a*, for any ratio of the radii R_1 and R_2.

For very small ratios R_2/R_1, i. e. for $R_2 \to 0$, one finds from Eq. (59) that $v^{\,\mathrm{nl}} \to N_1 b_{11}\,[1 - \frac{3}{4}N_2/(N_1+N_2)]$. This yields the maximum density $\max(\hat{n}_1^{\,\mathrm{nl}}) = 4/b_{11}$ for $N_2 \gg N_1$. Thus, $\hat{n}_1^{\,\mathrm{nl}}$ exceeds the maximum density of the linear approximation or of the corresponding one-component VdW gas, $\max(\hat{n}_{1,1}^{\,\mathrm{lin}}) = \max(n_1^{\,\mathrm{oc}}) = 1/b_{11}$, by a factor of four in this case.

Note that the value $4/b_{11}$ appears in the linear approximation as well: For $v_2^{\,\mathrm{lin}} \to V$, it is $\max(\hat{n}_{1,2}^{\,\mathrm{lin}}) = 4/b_{11}$ at $n_2 = 0$, but this density cannot be achieved because $p_1^{\,\mathrm{lin}}(n_1, n_2)$ is infinite for $n_1 \ge 1/b_{11}$.

Let us consider now the consequences of negative derivatives $\partial p^{\,\mathrm{nl}}/\partial N_2 < 0$ in the non-linear approximation. If a negative $\partial p^{\,\mathrm{nl}}/\partial N_2$ occurs for a density $n_1' = \mathrm{const.}$ at $n_2 = 0$, the pressure $p^{\,\mathrm{nl}}(n_1', n_2)$ has a minimum at a certain density $n_{2,\,\min} > 0$ which is determined by the boundary $\hat{n}_1^{\,\mathrm{nl,\,bd}}(n_2)$. For increasing n_1 along the boundary, consequently, the non-linear pressure is always lower than that for increasing n_1 at fixed $n_2 = 0$. Hence, higher densities can be achieved along the boundary, in particular, $n_1 > 1/b_{11}$.

Therefore, exceeding $n_1^{\,\mathrm{nl}} = 1/b_{11}$ requires that the boundary starts inside the the non-linear domain at $n_2 = 0$. Thus, the condition $\hat{n}_1^{\,\mathrm{nl,\,bd}}(0) < 1/b_{11}$ provides the critical radius $R_{2,\,\mathrm{crit}}$ (23),

$$b_{11} < 2b_{12} \quad \rightsquigarrow \quad R_{2,\,\mathrm{crit}}(R_1) = (\sqrt[3]{4} - 1)\,R_1 \; . \tag{65}$$

On the other hand, the boundary starts at $n_1 = 8/(14\,b_{11})$ for $R_2 \to 0$ at $n_2 = 0$, i. e., for any density $b_{11}n_1 \le 8/14 \approx 1/2$, negative values of $\partial p^{\,\mathrm{nl}}/\partial N_2$ do not occur for any radii.

Although it is pathological that the non-linear pressure firstly decreases for high densities n_1, if particles of the second and smaller component are added to the system, there is a reasonable explanation for the lowered pressure along boundary (64) for small radii $R_2 < R_{2,\,\mathrm{crit}}$.

Consider, for instance, $n_1 b_{11} = 0.9$ in Fig. 1 (*a*). Since it is $R_2/R_1 = 0.4$, the dimensionless density of the small particles at the boundary $\hat{n}_1^{\,\mathrm{nl,\,bd}}(n_2)$ nearly vanishes, $n_2 b_{22} \approx 0.05$, whereas the absolute amounts of the small and large particles are about equal. For the excluded volume interaction of the large particles in the pressure formula (16), therefore, the influence of the mixed term b_{12} becomes comparable to that of the distinctly larger non-mixed term b_{11}.

For $R_2/R_1 \ll 1$, one obtains $n_2 \gg n_1$ near the boundary at $n_1 b_{11} = 0.9$, i. e. the large particles are completely surrounded by the smaller particles and interact mostly with these but hardly with other large particles anymore. In this situation, consequently, the excluded volume interaction of the large particles is governed by the essentially smaller b_{12} and not by $b_{11} \le 8\,b_{12}$.

One might interpret this behavior as an effective attraction between small and large particles, but it is rather a strong reduction of the large particles' excluded volume suppression.

As VdW approximations are low-density approximations, they coincide for these densities, but they evidently become inadequate near the limiting densities: both the discussed formulations do evidently not match the real gas of rigid spheres there.

For high densities, the linear approximation behaves natural, i. e. it is $\partial p^{\,\mathrm{lin}}/\partial N_q > 0$ always. However, one has to introduce the additional terms $\tilde{b}_{12}$ and $\tilde{b}_{21}$. For choice (20), these terms provide a one-component-like behavior in the limits $R_2 = R_1$ and $R_2 = 0$, but they have no concrete physical meaning.

In the non-linear approximation, there occur pathologic pressure derivatives $\partial p^{\,\mathrm{nl}}/\partial N_2 < 0$ for $R_2 \ll R_1$. However, the non-linear formulae may be used for special purposes, e.g., for $n_1 > 1/b_{11}$ at intermediate $n_2 b_{22}$, where the linear approximation is yet invalid.

APPENDIX B: Stability of the Non-linear Approximation

The non-linear enhancement in the GCE or the occurence of negative values for $\partial p^{\,\mathrm{nl}}/\partial N_q$ in the CE suggests a further investigation concerning the thermodynamical stability of the non-linear approximation.

One can readily check that, in the CE, $\partial p^{\,\mathrm{nl}}/\partial V < 0$ generally, so there is no mechanical instability. To investigate whether there is a chemical instability [24], it is necessary to study partial derivatives with respect to the particle numbers, $\partial/\partial N_q$, of the chemical potentials

$$\mu_p(T, V, N_1, N_2) \quad \equiv \quad -T\,\tfrac{\partial}{\partial N_p}\,\ln[Z(T, V, N_1, N_2)] \; . \tag{66}$$

Partial derivatives of the pressure with respect to the particle numbers $\partial p/\partial N_q$ have no relevance here.

For the examination of chemical stability, it is appropriate to switch from the free energy of the CE, $F(T, V, N_1, N_2) \equiv -T\,\ln[Z(T, V, N_1, N_2)]$, to the Gibbs free energy or free enthalpy

$$G(T, p, N_1, N_2) \quad \equiv \quad F + p\,V = \mu_1 N_1 + \mu_2 N_2 \; , \tag{67}$$

where $\mu_q(T, p, N_1, N_2) \equiv \partial G/\partial N_q$. This requires that $p(T, V, N_1, N_2)$ can be solved for $V(T, p, N_1, N_2)$, which is the case for the non-linear approximation,

$$V^{\,\mathrm{nl}}(T, p, N_1, N_2) = \tfrac{N_1+N_2}{p/T} + N_1 b_{11} + N_2 b_{22} - \tfrac{N_1\,N_2}{N_1+N_2} D.$$

Further, it is useful to introduce the molar free enthalpy $g \equiv G/(N_1+N_2) = g(T,p,x_1)$ with the molar fractions $x_1 \equiv N_1/(N_1+N_2)$ and $(1-x_1) = x_2 \equiv N_2/(N_1+N_2)$ of components 1 and 2, respectively. Then the chemical stability of a binary mixture [24] corresponds to the condition

$$\frac{\partial^2}{\partial x_1^2}\, g(T,p,x_1) = \frac{\partial \mu_1(T,p,x_1)}{\partial x_1} - \frac{\partial \mu_2(T,p,x_1)}{\partial x_1} > 0\ . \tag{68}$$

For the non-linear approximation, one obtains

$$g^{\,\mathrm{nl}}(T,p,x_1) = x_1 \left\{ T \ln\left[\frac{x_1}{\phi_1}\,\frac{p}{T}\right] + p\ \ b_{11} - (1-x_1)^2 \times \right.$$

$$\left. \times D) \quad + (1-x_1) \left\{ T \ln\left[\frac{1-x_1}{\phi_2}\,\frac{p}{T}\right] + p\ \ b_{22} - x_1^2 D\ \right\}, \right. \tag{69}$$

and thus condition (68) is satisfied:

$$\frac{\partial^2}{\partial x_1^2}\, g^{\,\mathrm{nl}}(T,p,x_1) = \frac{T}{x_1} + \frac{T}{1-x_1} + p\,2D > 0. \tag{70}$$

Therefore, the system described by the non-linear approximation is thermodynamically stable – despite the pathologic behavior in special cases. Due to the equivalence of the thermodynamical ensembles, this is true for any representation of the model.

APPENDIX C: Two VdW Approximations in the GCE

In this part, we will study the non-linear and linear approximations in the grand canonical ensemble. As in the CE, the differences between the linear and non-linear approximations occur only for the high densities of larger particles n_q which correspond to large chemical potentials μ_q in the grand canonical treatment. Therefore, we will study the limit given by Eq. (43): $\mu_1/T \to \infty$ for constant T, μ_2 and $R_2 \le R_1$, where $\xi_1 \to \infty$.

The transcendental exponents of both approximations contain an attractive part besides the usual VdW-like suppressive part $\exp[-(p/T)\, b_{qq}]$: In the linear approximation (35) and (36), the suppression is reduced, but the transcendental exponents are always negative – whereas the suppression in the non-linear approximation (28) and (29) is not only reduced, but the transcendental exponent of ξ_2^{nl} can even become positive in the above limit.

To examine the latter, we rewrite the coupled transcendental equations (28) and (29) as

$$\xi_1^{\mathrm{nl}} = \phi_1 \exp\ \ \frac{\mu_1}{T}\ \ \times$$

$$\times \exp\ \ -\ \ \xi_1^{\mathrm{nl}} + \xi_2^{\mathrm{nl}}\ \ b_{11}\ \ \ 1 - \frac{D/b_{11}}{\left(\xi_1^{\mathrm{nl}}/\xi_2^{\mathrm{nl}}+1\right)^2}\ \ \ , \tag{71}$$

$$\xi_2^{\mathrm{nl}} = \phi_2 \exp\ \ \frac{\mu_2}{T}\ \ \times$$

$$\times \exp\ \ -\ \ \xi_1^{\mathrm{nl}} + \xi_2^{\mathrm{nl}}\ \ b_{22}\ \ \ 1 - \frac{D/b_{22}}{\left(1+\xi_2^{\mathrm{nl}}/\xi_1^{\mathrm{nl}}\right)^2}\ \ \ . \tag{72}$$

If R_2 is sufficiently smaller than R_1, then D/b_{22} is larger than unity, and the transcendental exponent of ξ_2^{nl} (72) can become positive,

$$0 < \frac{D}{b_{22}} - \ \ 1 + \frac{\xi_2^{\mathrm{nl}}}{\xi_1^{\mathrm{nl}}}\ \ ^2 \iff \frac{\xi_2^{\mathrm{nl}}}{\xi_1^{\mathrm{nl}}} < a_2 \equiv \sqrt{\frac{D}{b_{22}}} - 1. \tag{73}$$

The coefficient $a_2 = a_2(R_1/R_2)$ introduced here is the crucial combination of excluded volumes in the non-linear approximation. It characterizes the behavior of this approximation in limit (43), i. e. for $\xi_1 \to \infty$.

For equal radii $R_2 = R_1$, it is $a_2 = -1$, and one has full VdW-like suppression, $\propto \exp[-(p/T)\, b_{qq}]$. Negative a_2 indicate the strength of suppression of ξ_2^{nl} for increasing ξ_1^{nl}. For $-1 < a_2 < 0$, the suppression is reduced, most strongly for $a_2 \approx 0$. In the case where $a_2 = 0$, there is no suppression in limit (43) but $\xi_2^{\mathrm{nl}} \to A_2 = \text{const.}$ for $\xi_1^{\mathrm{nl}} \to \infty$. Thus, the condition $a_2 = 0$ provides the critical radius,

$$D/b_{22} = 1 \quad \Longleftrightarrow \quad R_{2,\,\mathrm{crit}} = (\sqrt[3]{4} - 1)\, R_1\ , \tag{74}$$

which coincides with the canonical result (65).

For positive a_2 or $R_2 < R_{2,\,\mathrm{crit}}$, the non-linear enhancement occurs: ξ_2^{nl} is enhanced by increasing ξ_1^{nl} as long as the second exponent in (72) is positive, i. e. for $\xi_2^{\mathrm{nl}} < a_2\, \xi_1^{\mathrm{nl}}$. The transcendental factor of ξ_1^{nl} (71) has only a reduced suppression in this case. According to Eq. (73), one obtains

$$\xi_2^{\mathrm{nl}} \to a_2\, \xi_1^{\mathrm{nl}}\ , \qquad \text{but also} \qquad n_2^{\mathrm{nl}} \to a_2\, n_1^{\mathrm{nl}}\ , \tag{75}$$

since $n_2^{\mathrm{nl}}/n_1^{\mathrm{nl}} = \xi_2^{\mathrm{nl}}/\xi_1^{\mathrm{nl}}$ due to Eqs. (32) and (33).

Using Eqs. (75) and (73), one obtains for the particle densities (32) and (33)

$$n_1^{\mathrm{nl}} \to \frac{1}{b_{11} - a_2^2\, b_{22}} = \frac{1}{b_{11} - (\sqrt{D} - \sqrt{b_{22}}\,)^2}, \tag{76}$$

$$n_2^{\mathrm{nl}} \to a_2\, n_1^{\mathrm{nl}} \to \frac{a_2}{b_{11} - a_2^2\, b_{22}} = \frac{\sqrt{b_{22}}}{b_{22}}\, \frac{\sqrt{D} - \sqrt{b_{22}}}{b_{11} - (\sqrt{D} - \sqrt{b_{22}}\,)^2}. \tag{77}$$

It is clearly seen that the density n_1^{nl} can exceed $1/b_{11}$ for positive a_2. As in the CE, the maximum value, $\max(n_1^{\mathrm{nl}}) = 4/b_{11}$, is achieved for $R_2 = 0$ or $a_2 = \infty$. Then, in limit (43), the density of the second component diverges, $n_2^{\mathrm{nl}} \to \infty$, but its total excluded volume vanishes, $n_2^{\mathrm{nl}}\, b_{22} \to 0$, as seen from Eq. (77).

There is yet another case where condition (73) is fulfilled, the early enhancement: ξ_2^{nl} can be enhanced with increasing μ_2 for constant T and μ_1, if μ_1 is sufficiently large. This enhancement takes place only at small μ_2, and it obviously vanishes when μ_2 is large enough so that $\xi_2^{\mathrm{nl}} \ge a_2 \xi_1^{\mathrm{nl}}$. The early enhancement is the direct analog to a negative derivative $\partial p^{\,\mathrm{nl}}/\partial N_q < 0$ in the CE.

The coupled transcendental equations of the linear approximation (35) and (36) may be rewritten similarly to Eqs. (71) and (72). For choice (20), one obtains, in terms of D from Eq. (15):

$$\xi_1^{\mathrm{lin}}(T,\mu_1,\mu_2) = A_1 \times$$

$$\times \exp\ \ -\ \ \xi_1^{\mathrm{lin}} + \xi_2^{\mathrm{lin}}\ \ b_{11}\ \ \ 1 - \frac{\xi_2^{\mathrm{lin}}}{\xi_1^{\mathrm{lin}} + \xi_2^{\mathrm{lin}}}\, \frac{D}{b_{11} + b_{22}}\ \ \ , \tag{78}$$

$$\xi_2^{\mathrm{lin}}(T,\mu_1,\mu_2) = A_2 \times$$

$$\times \exp\ \ -\ \ \xi_1^{\mathrm{lin}} + \xi_2^{\mathrm{lin}}\ \ b_{22}\ \ \ 1 - \frac{\xi_1^{\mathrm{lin}}}{\xi_1^{\mathrm{lin}} + \xi_2^{\mathrm{lin}}}\, \frac{D}{b_{11} + b_{22}}\ \ \ . \tag{79}$$

In this case, the condition for the enhancement of ξ_2^{lin} for $R_2 \le R_1$ would be

$$\frac{\xi_2^{\mathrm{lin}}}{\xi_1^{\mathrm{lin}}} < \tilde{a}_2 \equiv -\frac{2 b_{12}}{b_{11} + b_{22}}\ . \tag{80}$$

As $\tilde{a}_2$ is always negative, the VdW-like suppression is only reduced in this approximation. Like in the non-linear approximation, $\tilde{a}_2 = -1$ corresponds to equal radii $R_2 = R_1$

and the full VdW-like suppresion, whereas $\tilde{a}_2 = -1/4$ ($R_2 = 0$) corresponds to the most strongly reduced suppresion in the linear approximation.

Thus, the densities $n_q^{\rm lin}$ can not exceed the maximum value $1/b_{qq}$ of the corresponding one-component case. Furthermore, the density $n_2^{\rm lin}$ (40) vanishes in the analogous limit to (43), $\xi_1^{\rm lin} \to \infty$, in contrast to the non-linear behavior.

In the case $R_1 \leq R_2$, one would evidently investigate the coefficients $a_1 \equiv (\sqrt{D/b_{11}} - 1)$ in the non-linear approximation and $\tilde{a}_1 \equiv -(2b_{12})/(b_{11} + b_{22}) = \tilde{a}_2$ in the linear one, respectively.

1. H. Stöcker, W. Greiner, and W. Scheid, Z. Phys. A **286**, 121 (1978); H. Stöcker and W. Greiner, Phys. Rep. **137**, 277 (1986); C. Greiner and H. Stöcker, Phys. Rev. D **44**, 3517 (1991).
2. P. Koch, B. Müller, and J. Rafelski, Phys. Rep. **142**, 167 (1986); J. Letessier, A. Tounsi, U.W. Heinz, J. Sollfrank, and J. Rafelski, Phys. Rev. Lett. **70**, 3530 (1993).
3. J. Cleymans and H. Satz, Z. Phys. C **57**, 135 (1993); J. Cleymans and K. Redlich Phys. Rev. Lett. **81**, 5284 (1998).
4. P. Braun-Munzinger, J. Stachel, J.P. Wessels, and N. Xu Phys. Lett. B **344**, 43 (1995) and B **365**, 1 (1996).
5. F. Becattini and U.W. Heinz, Z. Phys. C **76**, 269 (1997).
6. G.D. Yen, M.I. Gorenstein, W. Greiner, and S.N. Yang, Phys. Rev. C **56**, 2210 (1997).
7. Proceedings of the Quark Matter '96, Nucl. Phys. A **610**, 1c (1996).
8. P. Braun-Munzinger, I. Heppe, and J. Stachel, Phys. Lett. B **465**, 15 (1999).
9. J.D. van der Waals, Z. Phys. Chem. **5**, 133 (1889).
10. H.A. Lorentz, Ann. Physik **12**, 127 (1881).
11. D. Berthelot, Compt. Rend. **126**, 1703 and 1857 (1898).
12. A. Münster, *Statistical Thermodynamics* Vol. II (Springer, Heidelberg, 1974).
13. M.I. Gorenstein, A.P. Kostyuk and Y.D. Krivenko J. Phys. G **25**, L75 (1999).
14. K.A. Bugaev, M.I. Gorenstein, H. Stöcker, and W. Greiner, Phys. Lett. B **485**, 121 (2000).
15. F. Karsch, E. Laermann, P. Petreczky, and S. Stickan, Nucl. Phys. Proc. Suppl. **106**, 510 (2002).
16. M. Asakawa, T. Hatsuda, and Y. Nakahara, Nucl. Phys. A. **715**, 863 (2003).
17. K.A. Bugaev, Phys. Rev. C **76**, 014903 (2007).
18. K.A. Bugaev, Preprint **nucl-th/0611102** (2006).
19. G. Zeeb, Diploma thesis, *Zweikomponentige Vander-Waals-Zustandsgleichungen mit relativistischen Eigenvolumentermen für das hadronische Gas* (Frankfurt am Main, 2002).
20. K.A. Bugaev, M.I. Gorenstein, I.N. Mishustin, and W. Greiner, Phys. Rev. **C62**, 044320 (2000); Phys. Lett. **B 498**, 144 (2001) and references therein.
21. K.A. Bugaev, Acta. Phys. Polon. B **36**, 3083 (2005); Preprint **nucl-th/0507028**.
22. K.A. Bugaev, Nucl. Phys. A **606**, 559 (1996); K.A. Bugaev, M.I. Gorenstein, and W. Greiner, J. Phys. G **25**, 2147 (1999) and Heavy Ion Phys. **10**, 333 (1999).
23. V.K. Magas *et al.*, Nucl. Phys. A **661**, 596 (1999); C. Anderlik *et al.*, Phys. Rev. C **59**, 3309 (1999).
24. L.E. Reichl, *A Modern Course in Statistical Physics* (Wiley, New York, 1998).

Received 17.09.07

РІВНЯННЯ СТАНУ ДВОКОМПОНЕНТНОГО ГАЗУ ВАН-ДЕР-ВААЛЬСА З РЕЛЯТИВІСТСЬКИМИ ВИКЛЮЧЕНИМИ ОБ'ЄМАМИ

Г. Зеєб, К.О. Бугаєв, П.Т. Ройтер, Х. Штьокер

Р е з ю м е

Отримано канонічну статистичну суму для моделі двокомпонентного виключеного об'єму, яка веде до двох різних рівнянь Ван-дер-Ваальса. Одне з рівнянь відоме як суміш Лоренца–Бертелло, а інше було запропоновано недавно. Обидві моделі проаналізовано в канонічному та великому канонічному ансамблях. Пригнічення щільності частинок в цих двокомпонентних формулюваннях послаблено порівняно з моделлю Ван-дер-Ваальса з однокомпонентним виключеним об'ємом, але двома істотно різними способами. Багатокомпонентні моделі, які використовуються в наш час, не мають такого послаблення. Як нами показано, такі моделі неправильні, якщо використовуються для сумішей частинок з різними радіусами твердого кора. Для високих температур взаємодію твердого кора покращено шляхом врахування лоренцева скорочення сферичних виключених об'ємів частинок, яке веде до помітного посилення внесків легких частинок в термодинамічній функції. Результуючий вплив двох радіусів твердого кора і лоренцева скорочення на вихід піонів та нуклонів детально вивчено на АГС- та СПС-даних.